JCTC Journal of Chemical Theory and Computation

Article

pubs.acs.org/JCTC

The *GW*-Method for Quantum Chemistry Applications: Theory and Implementation

M. J. van Setten,*[,†] F. Weigend,[†,‡] and F. Evers[†,¶]

[†]Institute of Nanotechnology, Karlsruhe Institute of Technology, P.O. Box 3640, D-76021 Karlsruhe, Germany

[‡]Institute of Physical Chemistry, Karlsruhe Institute of Technology, P.O. Box 3640, D-76021 Karlsruhe, Germany

[¶]Institute of Theoretical Condensed Matter, Karlsruhe Institute of Technology, P.O. Box 3640, D-76021 Karlsruhe, Germany

Supporting Information

ABSTRACT: The *GW*-technology corrects the Kohn−Sham (KS) single particle energies and single particle states for artifacts of the exchange-correlation (XC) functional of the underlying density functional theory (DFT) calculation. We present the formalism and implementation of *GW* adapted for standard quantum chemistry packages. Our implementation is tested using a typical set of molecules. We find that already after the first iteration of the self-consistency cycle, G_0W_0, the deviations of quasi-particle energies from experimental ionization potentials and electron affinities can be reduced by an order of magnitude against those of KS-DFT using GGA or hybrid functionals. Also, we confirm that even on this level of approximation there is a considerably diminished dependency of the G_0W_0-results on the XC-functional of the underlying DFT.

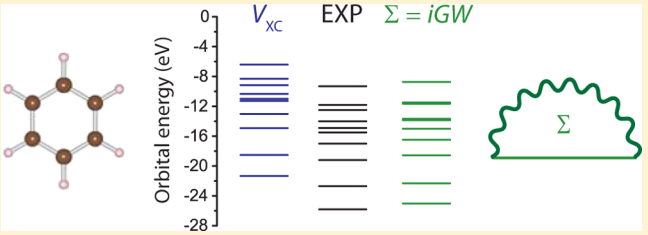

1. INTRODUCTION

One of the most used approaches for the computational study of solids, nanoscale systems, and molecules is the density functional theory (DFT).[1] DFT has an ubiquitous appearance in computational chemistry and materials sciences because it often offers the only possibility to obtain useful ab initio results for relevant system sizes.

A well-known difficulty with DFT-calculations is related to approximations in the exchange-correlation (XC) functional, the most familiar one being the local density approximation (LDA).[2,3] The use of such local (or semilocal) approximations has several important consequences, *in praxi*. First, the neglect of the derivative-discontinuity in such approximate functionals implies uncertainties in the description of charge-transfer processes, because the alignment of Kohn−Sham (KS) levels of different subsystems is not properly accounted for. Second, neglecting nonlocal terms also implies that weak, van der Waals like, binding forces are being described badly or not at all. Moreover, (differences between) KS-single particle energies are often interpreted as physical excitation energies, because the KS-estimates of these energies tend to compare significantly better to experimental results than, for instance, those originating from Hartree−Fock (HF) theory. Still, a formal justification for this praxis (i.e., a KS-analog of the Koopmans' theorem[4]) does not exist in general. To identify situations when good quantitative estimates can be obtained, nevertheless, is the subject of ongoing research.[5,6]

A method to systematically improve upon shortcomings of DFT-estimates of single particle excitation spectra, i.e., ionization potentials and electron affinities, is well established for electronic band structure calculations in solids: the *GW*-method. Its central object is the Green's function G; its poles describe single particle excitation energies and lifetimes. The *GW*-approach is based on an exact representation of G in terms of a power series of the screened Coulomb interaction W, which is called the *Hedin equations*.[7,8] The *GW*-equations are obtained as an approximation to the Hedin-equations, in which the screened Coulomb interaction W is calculated neglecting so-called *vertex corrections*.[9−12]

Effectively, one can say that the *GW*-approach, similar to other one electron Green's function approaches, replaces in the DFT-calculation the problematic unknown XC-potential by a *self-energy*, Σ. In this process the KS-equations are transformed into a self-consistent set of *quasi-particle* equations. Similar to the XC-potentials of DFT, which are functionals of the electron density, $\Sigma[G]$ is a functional of G and therefore typically needs to be updated in the iteration cycle that solves the quasi-particle equations. In contrast to XC-potentials, Σ is not Hermitian and depends on energy. Furthermore similar to the Fock-operator and unlike (semi) local XC-potentials, Σ is nonlocal in space.

A key feature of Green's functions is that their poles by construction *define* the single-particle (or quasi-particle) excitation energies. In particular, the *GW*-quasi-particle energies up to the highest occupied molecular orbital (HOMO) correspond to the primary vertical ionization energies. When using a basis that keeps track explicitly also of core states, we have access to the ionization energies relevant for core-level spectroscopies. The knowledge of the full quasi-particle spectrum and quasi-particle states also gives access to calculating other physical

Received: July 25, 2012
Published: November 5, 2012

   dx.doi.org/10.1021/ct300648t | *J. Chem. Theory Comput.* 2013, 9, 232−246

quantities. One example is molecular transport; another one is the calculation of optical excitation spectra via the solution of the Bethe-Salpeter equation (BSE).[11] Finally, also total energy calculations for structure relaxations can be performed with knowledge of G and W.[13]

Due to its quantitative success, the *GW*-method is about to become a standard tool to investigate band structures of solids and surfaces.[11] It is well-known that, and understood why, the gaps calculated from KS-DFT energies systematically underestimate the experimental values by up to 5 eV.[9,14,15] The *GW*-method, on the other hand, predicts for a large range for semiconductors the fundamental bandgap correctly up to a few tenths of an eV.[9,16−18] In some cases the results obtained from DFT are even qualitatively wrong. For instance Germanium, Indiumarsenide, and Ytriumhydride are predicted to be metallic by DFT where *GW* correctly predicts a finite gap.[9,19,20] Also for metallic systems the *GW*-method improves the description of the electronic structure significantly as compared to KS-DFT. For example, the bandwidths, relative positions of s- and d-states and the magnetic moments of transition metals have been shown to be described much better in the *GW*-framework than in that of KS-DFT.[21] Moreover, very recent studies showed that, if pseudo potential issues and relativistic effects are taken into account properly, *GW* also reproduces the band-structure of a heavy elements like gold and plutonium very accurately.[22,23] This promising potential has led to an active development, and recently the method has become available in various first principles solid state codes.[24−29]

Developments in this field are ongoing. A central step in the calculation of the *GW*-self-energy matrix elements needed to obtain the quasi-particle energies involves a sum over occupied as well as a sum over unoccupied orbitals. Several groups are exploring techniques to circumvent the later by replacing it by an identity minus a second sum over the occupied orbitals.[30,31] Ultimately this so-called "collapsing of the spectral sum" should lead to an improved scaling of the computational cost with the system size. A *GW*-calculation usually starts from the results of a DFT-calculation to which then in the *GW*-step corrections are being calculated. These corrected results may then be iterated to self-consistency. Some groups are therefore focusing at defining the optimal functional for the initial DFT-calculation.[32] For a *GW*-calculation the initial guess for the electronic response of the system is one of the most important input parameters to be obtained from the initial DFT-calculation. This is however not necessarily described best by a functional designed to perform well at describing the total energy and atomic structure, for which most regularly used functionals have been designed. A final important development mentioned here is involved with improving the core and semicore treatment.[32] As in DFT-calculations, it is also in a *GW*-calculation possible to treat the core levels of the atoms only approximately. This has to be done however with great care since they do contribute to the electronic response, which is needed in *GW* to calculate the screening.[34]

Several recent applications suggest that *GW* will also be successful when applied to single molecules. Examples are *GW*-studies on organic molecules,[35−42] CdSe clusters of up to 82 atoms,[43,44] hydrogen passivated Si clusters of up to 41 silicon atoms,[45] metal clusters,[46−49] and C_{60}.[50] In all cases ionization energies and electron affinities are calculated with an accuracy at least an order of magnitude closer to the experimental values than those that can be obtained from the KS-DFT energies. For optical excitation spectra,[43,45] quantitative and even qualitative improvements with respect to TDDFT have been observed by using GW+BSE. Moreover, first investigations as to the effect of self-consistency have demonstrated for small molecules that even further improvements are possible.[38,46,51,52] A special field where *GW*-studies on molecular clusters have proven useful is that of Molecular Electronics. Here special purpose tools are being developed to calculate transport properties of single molecules based on a *GW*-description of the electronic structure.[53,54]

Until recently many *GW*-studies on molecules employed band-structure codes and supercells, so only relatively small system sizes were accessible. The first applications using a localized basis set[37,46] date back less than ten years, and only very recently this is becoming a more applied approach.[38−41,52,55,56] However, to our knowledge there is until now only one multipurpose first principles package available that also offers the possibility to calculate the quasi-particle spectrum of molecular systems; the FHI-aims code.[52,57]

In this paper we describe how to build the G_0W_0-approach into a typical quantum chemistry package, operating with localized basis sets. A special feature of this implementation is the use of spectral representations of the response function. The use of spectral representations was formally introduced by Hedin,[9] and later applied by Tiago et al.[58] and very recently also by Bruneval.[56] In this way an analytic evaluation of energy integrals and derivatives is feasible. The matrix elements of Σ will be expressed via two electron integrals, which are often available in standard codes. Therefore, the resulting expressions can be implemented efficiently in any generic quantum chemistry code. To be specific, we give an example and describe our implementation into the TURBOMOLE package. Benchmark calculations have been performed using this implementation and will be discussed.

2. FORMALISM

2.1. Hedin Equations. In this section we recall the basic formalism behind the *GW*-approach. Its central object is the causal Green's function G. It is a matrix that depends on two spatial and two time coordinates; the corresponding matrix elements in space-time representation read $G(\mathbf{r}_1t_1,\mathbf{r}_2t_2)$. They represent the probability amplitude for a particle that has been created at $(\mathbf{r}_2t_2)$ in space time to be picked up at the point $(\mathbf{r}_1t_1)$. To simplify the notation, we adopt the convention that the combined coordinate $(\mathbf{r}_it_i)$ is replaced by the index i, so the matrix elements become $G(1,2)$. These matrix elements can be obtained from solving a set of coupled integral equations, the *Hedin* equations:[7,8]

$$G(1,2) = G_{\mathrm{H}}(1,2) + \int d(34) G_{\mathrm{H}}(1,3)\Sigma(3,4)G(4,2) \tag{1}$$

$$\Sigma(1,2) = i\int d(34) G(1,3^+)W(1,4)\Gamma(3,2,4) \tag{2}$$

$$W(1,2) = v(1,2) + \int d(34) v(1,3)P(3,4)W(4,2) \tag{3}$$

$$P(1,2) = -i\int d(34) G(1,3)\Gamma(3,2,4)G(4,1^+) \tag{4}$$

$$\Gamma(1,2,3) = \delta(1-2)\delta(2-3) + \int d(4567)\frac{\delta\Sigma(1,2)}{\delta G(4,5)} \times G(4,6)G(7,5)\Gamma(6,7,3) \tag{5}$$

dx.doi.org/10.1021/ct300648t | J. Chem. Theory Comput. 2013, 9, 232−246

The integrands are summations over spatial and time coordinates. The superscript plus $^+$ indicates a positive infinitesimal added to the time variable.

Equations 1−5 constitute a complicated self-consistency problem for the matrix G and the matrix operator Γ. The first of these equations, 1, is the *Dyson equation*. It is the basic statement that will eventually translate into the quasi-particle equation. The Green's function G_H, which appears here as reference Green's function, is to be taken with respect to the Hartree-ground state. (G_H should be distinguished from the initial guess G_{in} for G needed later when iteratively solving this self-consistency problem.[89] This initial guess will be the Green's function with respect to the KS-ground state: $G_{in} = G_{KS}$.) The basic structure of the Dyson equation is transparent: it features two Green's functions describing the ingoing and outgoing states of particles that scatter with a strength described by the self-energy Σ. The second equation, 2, defines Σ in terms of the dynamically screened Coulomb interaction W and the vertex operator Γ. These two objects are given by the consecutive three equations. Equation 3 is the standard expression relating the screened interaction to the Coulomb interaction $v(\mathbf{r}_1\mathbf{r}_2) = e^2/(\mathbf{r}_1 - \mathbf{r}_2)$ and the polarization function P given in eq 4.

Upon approximating the vertex function, Γ, by the first term of 5 we can close the set of eqs 1−4. In this way we arrive at the *GW*-method. To obtain an exact solution, the second term in the last equation would have to be kept and iterated as well. This last equation, 5, is the *Bethe-Salpeter* equation. It takes into account all those multiscattering events, that cannot be accounted for by the effective, retarded interaction W, alone. Its solution is difficult, because Γ is a matrix-operator. Moreover, no particular means exists to evaluate the functional derivative making the exact solution impossible.

From a computational point of view, eq 3 is slightly inconvenient because to solve it requires an inversion. This becomes particularly obvious when casting 3 into a familiar form featuring the dielectric function

$$W(1, 2) = \int d(3)\epsilon^{-1}(1, 3)v(3, 2) \tag{6}$$

$$\epsilon(1, 2) = \delta(1, 2) - \int d(3)v(1, 3)P(3, 2) \tag{7}$$

Fortunately, in many quantum chemistry codes this inversion already is implemented. Namely, to determine optical excitation spectra, where the full density response χ is required. It relates to P and ϵ in the following way:

$$\chi(1, 2) = P(1, 2) + \int d(34)P(1, 3)v(3, 4)\chi(4, 2) \tag{8}$$

$$\epsilon^{-1}(1, 2) = \delta(1, 2) + \int d(3)v(1, 3)\chi(3, 2) \tag{9}$$

Therefore, it is convenient to express W also in terms of the χ (the reducible response function):

$$W(1, 2) = v(1, 2) + \int d(34)v(1, 3)\chi(3, 4)v(4, 2) \tag{10}$$

The full density response χ is a central object of time-dependent DFT. As it turns out, for this reason an approximate expression for χ is readily available in many quantum chemistry codes that offer calculations of optical excitations.

2.2. Dyson Equation and Quasi-Particles. *2.2.1. Separation of Time Scales and Poles of the Green's Function.* In a gas of N noninteracting fermions each single particle orbital $\psi_n^{(0)}(\mathbf{r})$ corresponds to a quantum number n with an associated energy $\epsilon_n^{(0)}$ that are conserved. The fact that there are as many conserved quantities as there are particles makes the problem (relatively) easily tractable. Upon introducing an interaction between the particles, the situation becomes much more complicated because due to particle scattering almost all conservation laws are lost. Correspondingly, the interacting eigenstates can no longer be given by a single Slater determinant.

One may, however, ask how long it takes for the interaction to mix in other Slater determinants if the time evolution started with an initial state constructed from a single Slater determinant only. If the interaction is weak, then the mixing may take long enough so that it can be meaningful to introduce a concept of "approximate conservation laws", where an electron carries a given quantum number for a certain time τ_n before it is scattered into another state. Specifically, if a condition

$$\Delta_{n,n'} \gg \hbar/\tau_n, \hbar/\tau_{n'}, \qquad \Delta_{n,n'} = \epsilon_n - \epsilon_{n'} \tag{11}$$

is satisfied, then the lifetimes τ_n and $\tau_{n'}$ are long enough so that the wave function experiences in its time evolution a phase-shift with clearly identifiable contributions from pairs of neighboring in energy "quasi-particle" states n and n'. In this situation one can separate a "short time dynamics", completely governed by the quasi-particle energies ϵ_n, from a long time dynamics, $t \gg \tau_n$, where the decay processes can enter.

In the presence of a separation of time scales the concept of Green's functions, G, is particularly helpful. By definition,[59] Green's functions formally are expectation values taken with respect to the interacting ground state. Since the Hamiltonian does not depend on time explicitly, this results in time translational invariance and the matrix elements depend only on the difference of two times: $G(\mathbf{r}_1,\mathbf{r}_2;t_1 - t_2)$. Hence, an equivalent representation of G can be given in Fourier/energy space

$$G(t_1 - t_2) = \int_{-\infty}^{\infty} \frac{dE}{2\pi} e^{-iE(t_1-t_2)}G(E) \tag{12}$$

(Here and in the following we measure an action in units of $\hbar$; effectively $\hbar \to 1$.)

Per constructionem, the poles of G in the frequency plane, $z_n = \epsilon_n + i\gamma_n$, correspond to the quasi-particle energies and their (single particle) life times $\gamma_n = 2\pi/\tau_n$. For noninteracting particles, these poles are situated infinitely close to the real axis, $z_n^{(0)} = \epsilon_n^{(0)} - i\eta\mathrm{sgn}(\epsilon_n^{(0)} - \mu)$, since there is no scattering and the associated quantum numbers are conserved. We have introduced the chemical potential μ and a positive real number η which is to be sent to zero, $\eta \to 0$, at the end of all calculations. As usual, μ controls the particle number via

$$N = \int_{-\infty}^{\mu} dE\ \mathrm{Tr}\, A(E) \tag{13}$$

$$A(E) = -\frac{1}{\pi}\mathrm{sgn}(E - \mu)\mathrm{Im}(G(E)) \tag{14}$$

where $A(E)$ denotes the "spectral function" and "Tr" a trace over the spatial degrees of freedom. The spectral function represents the full information content of the Green's function, as may be inferred from the Lehmann representation:[59,60]

$$G(E) = \int_{-\infty}^{+\infty} dE' \frac{A(E')}{E - E' + i\eta\mathrm{sgn}(E' - \mu)} \tag{15}$$

In the Green's function language, by switching on the interaction we shift the poles along the real axis and into the imaginary plane,

dx.doi.org/10.1021/ct300648t | J. Chem. Theory Comput. 2013, 9, 232−246

into z_n. (Pole shiftings crossing the real axis are forbidden in the process due to causality.) Green's functions owe their popularity to the fact that they offer a concept to calculate these shifts (and other quantities) perturbatively in the interaction resumming partial series of infinitely many perturbative contributions.

2.2.2. Spectral Representation and Quasi-Particle Equation. The Dyson equation for $G(E)$, 1, can be rewritten in Fourier space. After analytic continuation into the complex frequency domain and recalling the representation of the (inverse of the) unperturbed Green's function

$$G_{\mathrm{H}}^{-1}(z) = z - H_{\mathrm{H}},\ z\epsilon\mathbb{C} \tag{16}$$

where H_{H} denotes the Hartree-Hamiltonian, we get

$$(z - H_{\mathrm{H}})\cdot G(z) - \Sigma(z)\cdot G(z) = 1 \tag{17}$$

We here suppress the spatial indices by applying a matrix notation where $A\cdot B$ stands for $\int A(\mathbf{r},\mathbf{r}'')B(\mathbf{r}'',\mathbf{r}')d\mathbf{r}''$ and AB for $A(\mathbf{r},\mathbf{r}')B(\mathbf{r},\mathbf{r}')$.[90]

A solution of the Dyson equation, 17, can be constructed by introducing a quasi-spectral representation:

$$G(\mathbf{r},\mathbf{r}';z) = \sum_n \frac{\Psi_{r,n}(\mathbf{r},z)\Psi_{l,n}^{\dagger}(\mathbf{r}',z)}{z - \varepsilon_n(z) + i\eta\mathrm{sgn}(\varepsilon_n - \mu)} \tag{18}$$

It features left and right eigenvectors, $\Psi_{l,n}(z)$, $\Psi_{r,n}(z)$, and eigenvalues $\varepsilon_n(z)$ that represent the quasi-particle/hole states $\Psi_n(z)$ and energies $\varepsilon_n(z)$. They are found as solutions of the quasi-particle equations

$$(H_{\mathrm{H}} + \Sigma(z))\cdot\Psi_{r,n}(z) = \varepsilon_n(z)\Psi_{r,n}(z) \tag{19}$$

$$\Psi_{l,n}^{\dagger}(z)\cdot(H_{\mathrm{H}} + \Sigma(z)) = \varepsilon_n(z)\Psi_{l,n}^{\dagger}(z) \tag{20}$$

2.2.3. Quasi-Particle Equation with Kohn−Sham Reference System. With an eye on computational applications, we next write the quasi-particle equations in a suitable single particle reference basis. There are two natural options for choosing such a basis. An obvious possibility would be to adopt the basis of eigenstates of the Hartree-Hamiltonian H_{H}. Another possibility are the eigenstates and energies of the KS-Hamiltonian $H_{\mathrm{KS}} = H_{\mathrm{H}} + V_{\mathrm{XC}}$. In this article we prefer the second choice because the KS-Green's function

$$G_{\mathrm{KS}}(\mathbf{r},\mathbf{r}';E) = \sum_n \frac{\psi_n(\mathbf{r})\psi_n^{*}(\mathbf{r}')}{E - \epsilon_n + i\eta\mathrm{sgn}(\epsilon_n - \mu)} \tag{21}$$

where the sum over n is over all, occupied and virtual, KS-orbitals, tends to be much closer to the fixed point Green's function of the GW-cycle than the Hartree-based Green's function G_{H}. Hence, we will design an approach where the KS-states ψ_n and energies ϵ_n represent the zeroth order approximation to the quasi-particle states, $\Psi_n^{(0)}(z) = \psi_n$, and energies, $\varepsilon_n^{(0)}(z) = \epsilon_n$, if z takes values close to a pole, $z - \varepsilon_n(z) \approx 0$. With this plan it is natural to expand the quasi-particle states in terms of the reference orbitals:

$$\Psi_{r,n}(\mathbf{r},z) = \sum_{\underline{n}} \mathcal{U}_{n,\underline{n}}(z)\psi_{\underline{n}}(\mathbf{r}) \tag{22}$$

As the first step in the approximation cycle, we operate with G_{KS}. In this spirit we later will only keep the leading term

$$\mathcal{U}_{n,\underline{n}}(\epsilon_{n'}) = \delta_{nn'}\delta_{n\underline{n}} + O(v) \tag{23}$$

In the ψ_n-basis the quasi-particle eq 19 can be rewritten in the following way, suppressing dependency on the z-coordinate in $\Sigma,\mathcal{U}$, ε_n:

$$\begin{aligned}
&H_{\mathrm{H}}\sum_{\underline{n}}\mathcal{U}_{n',\underline{n}}\psi_{\underline{n}}(\mathbf{r}) + \int d\mathbf{r}'\Sigma(\mathbf{r},\mathbf{r}')\sum_{\underline{n}}\mathcal{U}_{n',\underline{n}}\psi_{\underline{n}}(\mathbf{r}') = \varepsilon_{n'}\sum_{\underline{n}}\mathcal{U}_{n',\underline{n}}\psi_{\underline{n}}(\mathbf{r})\\
&\sum_{\underline{n}}\mathcal{U}_{n',\underline{n}}\Big[\int d\mathbf{r}\bar{\psi}_n(\mathbf{r})H_{\mathrm{H}}\psi_{\underline{n}}(\mathbf{r}) + \iint d\mathbf{r}d\mathbf{r}'\bar{\psi}_n(\mathbf{r})\Sigma(\mathbf{r},\mathbf{r}')\psi_{\underline{n}}(\mathbf{r}')\Big]\\
&\quad = \varepsilon_{n'}\sum_{\underline{n}}\mathcal{U}_{n',\underline{n}}\int d\mathbf{r}\bar{\psi}_n(\mathbf{r})\psi_{\underline{n}}(\mathbf{r})\\
&\sum_{\underline{n}}\mathcal{U}_{n',\underline{n}}\Big[\epsilon_n\delta_{n,\underline{n}} - \iint d\mathbf{r}d\mathbf{r}'\bar{\psi}_n(\mathbf{r})v_{xc}(\mathbf{r})\delta(\mathbf{r}-\mathbf{r}')\psi_{\underline{n}}(\mathbf{r}')\\
&\qquad + \iint d\mathbf{r}d\mathbf{r}'\bar{\psi}_n(\mathbf{r})\Sigma(\mathbf{r},\mathbf{r}')\psi_{\underline{n}}(\mathbf{r}')\Big]\\
&\quad = \varepsilon_{n'}\sum_{\underline{n}}\mathcal{U}_{n',\underline{n}}\delta_{n,\underline{n}}\\
&\sum_{\underline{n}}\mathcal{U}_{n',\underline{n}}(z)\Big[\epsilon_n\delta_{n,\underline{n}} + \iint d\mathbf{r}d\mathbf{r}'\bar{\psi}_n(\mathbf{r})(\Sigma(\mathbf{r},\mathbf{r}',z) - v_{\mathrm{xc}}(\mathbf{r})\delta(\mathbf{r}-\mathbf{r}'))\psi_{\underline{n}}(\mathbf{r}')\Big]\\
&\quad = \varepsilon_{n'}(z)\mathcal{U}_{n',n}(z)\\
&\sum_{\underline{n}}\mathcal{U}_{n',\underline{n}}(z)[\epsilon_n\delta_{n,\underline{n}} + \langle n|(\Sigma(z) - V_{\mathrm{xc}})|\underline{n}\rangle)] = \varepsilon_{n'}(z)\mathcal{U}_{n',n}(z)
\end{aligned} \tag{24}$$

where the full z-dependency has been restored in the last two lines. Equation 24 constitutes an eigensystem-problem. For a given value of z we are looking for the set of eigenvalues $\varepsilon_{n'}(z)$ and the belonging eigenvectors with components $\mathcal{U}_{n',n}(z)$ of the matrix in brackets, [...].[91]

The poles of the Green's function follow from the pole condition

$$z - \varepsilon_{n'}(z) = 0$$

Therefore, to find these poles we should solve the following self-consistency problem:

$$\sum_{\underline{n}}\mathcal{U}_{n',\underline{n}}(\varepsilon_{n'})\langle n|\Sigma(\varepsilon_{n'}) - V_{\mathrm{xc}}|\underline{n}\rangle = (\varepsilon_{n'} - \epsilon_n)\mathcal{U}_{n',n}(\varepsilon_{n'}) \tag{25}$$

This expression is the quasi-particle equation written with reference to the KS-system that we have been after. An analogue equation can also be written for the left-hand eigensystem

$$\sum_{\underline{n}}\tilde{\mathcal{U}}_{n',\underline{n}}(\varepsilon_{n'})\langle\underline{n}|\Sigma(\varepsilon_{n'}) - V_{\mathrm{xc}}|n\rangle = (\varepsilon_{n'} - \epsilon_n)\tilde{\mathcal{U}}_{n',n}(\varepsilon_{n'}) \tag{26}$$

where $\tilde{\mathcal{U}}_{n',\underline{n}}$ are the expansion coefficients of the left-hand eigenvectors in terms of the reference orbitals:

$$\Psi_{l,n}(\mathbf{r},z) = \sum_{\underline{n}}\tilde{\mathcal{U}}_{n,\underline{n}}(z)\bar{\psi}_{\underline{n}}(\mathbf{r}) \tag{27}$$

2.3. *GW*-Approximation. As indicated above, the GW-approximation ignores the second term in the RHS of eq 5. The expression for the self-energy becomes

$$\Sigma[G](1,2) = iG(1,2^{+})W(1,2^{+}) \tag{28}$$

in the energy domain

$$\Sigma[G](E) = \frac{i}{2\pi}\int_{-\infty}^{\infty} e^{-i\omega 0^{+}}G(E-\omega)W(\omega)d\omega \tag{29}$$

In our notation we keep the energy dependence explicit, E for fermionic and ω for bosonic degrees of freedom. Furthermore, by writing $\Sigma[G]$ we emphasize that in the GW-context $\Sigma[G]$ should be understood as a matrix functional of the Green's

dx.doi.org/10.1021/ct300648t | J. Chem. Theory Comput. 2013, 9, 232−246

function G. In the absence of vertex corrections also the equations for the screened interaction simplify considerably:

$$W(1,2) = v(1,2) + \int d(34)v(1,3)P(3,4)W(4,2) \tag{30}$$

$$P(1,2) = -iG(1,2)G(2,1^+) \tag{31}$$

Clearly, also $P[G]$ (and therefore W itself) should be viewed as functionals of G. Rephrasing the problem in terms of the full response function χ proceeds exactly in the same way as before. In frequency/real space domain we have the explicit representation

$$W(\mathbf{r}_1,\mathbf{r}_2;\omega) = v(\mathbf{r}_1-\mathbf{r}_2) + \int d\mathbf{r}_3 d\mathbf{r}_4 v(\mathbf{r}_1-\mathbf{r}_3)\chi(\mathbf{r}_3,\mathbf{r}_4;\omega)v(\mathbf{r}_4-\mathbf{r}_2) \tag{32}$$

$$\chi(\mathbf{r}_1,\mathbf{r}_2;\omega) = P(\mathbf{r}_1,\mathbf{r}_2;\omega) + \int d\mathbf{r}_3 d\mathbf{r}_4 P(\mathbf{r}_1,\mathbf{r}_3;\omega)v(\mathbf{r}_3-\mathbf{r}_4)\chi(\mathbf{r}_4,\mathbf{r}_2;\omega) \tag{33}$$

2.4. Self-Consistent Solutions of the *GW*-Equations. The ultimate task of a GW-calculation would be to find the matrix $G(E)$ that solves the GW-equations, i.e., the Dyson equation,

$$G = (G_H^{-1} - \Sigma[G])^{-1} \tag{34}$$

together with 28,30, and 31. Such a solution will be called "fully self-consistent".

Solving the GW-equations with full self-consistency has important advantages. Most notably, the self-consistent solution for $G(1,2)$ is generally not dependent on the reference system chosen in the Hedin equations.[61,62] This implies the following technical advantage. Starting from the initial guess G_{KS} the self-consistency iteration cycle is going to construct automatically the correct sequence of diagrams (in the Hartree-reference system) for the self-energy. The subtraction procedure ensures that the fixed point of this iteration does not depend on the choice of the initial functional. Recently, it was shown explicitly by Caruso et al. that both HF and KS-DFT as a starting point converge to the same self-consistent solution for various molecules.[61] Moreover, it has been shown by Tandetzky et al. that, although many self-consistent solutions exist in principle, there is only one physical solution.[62] This unique physical solution has also been shown to be the solution that is found by the commonly used algorithms.

Unfortunately, fully self-consistent solutions may be difficult to find and therefore not always affordable from the computational point of view. However, one could hope that for many practical purposes full self-consistency is not required in order to obtain a useful result. In such situations schemes providing "partial self-consistency" may be useful alternatives. [In addition different types of self-consistency, like Van Schilfgaarden's quasiparticle self-consistency, have been developed.][21]

2.4.1. Partial Self-Consistency: GW_0-Schemes. "Partially self-consistent" schemes that keep the screening fixed at that of the reference system – called GW_0 – have the formal definition

$$\Sigma[G](1,2) = iG(1,2^+)W_{ref}(1,2^+) \tag{35}$$

where W_{ref} is a screened Coulomb interaction that has been calculated once and for all for some reference system, which does not need to be the same as the one in the Hedin equations. In such schemes the iterative process of solving the GW-equations does not update W, instead it is kept fixed, $W = W_{ref}$. As a consequence, the fixed-point Green's function of the iteration cycle describes a gas of particles that interact with density fluctuations brought about by the reference system but not by itself. There are several possible choices for the reference system.

Screening Based on G_H: Hartree Approximation. One describes the dynamical screening of charges in the interacting electron gas on the time-dependent-Hartree level:

$$W_H(1,2) = v(1,2) + \int d(34)v(1,3)P_H(3,4)W_H(4,2) \tag{36}$$

$$P_H(1,2) = -iG_H(1,2)G_H(2,1^+) \tag{37}$$

In the constituting equation one makes the replacement $W_{ref} \to W_H$.

Screening Based on G_{KS}: DFT. The self-energy functional 35 replaces $W_{ref} \to W_{KS}$ where the KS-screened interaction is given by

$$W_{KS}(1,2) = v(1,2) + \int d(34)v(1,3)P_{KS}(3,4)W_{KS}(4,2) \tag{38}$$

$$P_{KS}(1,2) = -iG_{KS}(1,2)G_{KS}(2,1^+) \tag{39}$$

We mention that when working with DFT as the reference system, it can be convenient to re-express the Hartree-based Green's function: $G_H^{-1} = G_{KS}^{-1} + V_{XC}$.

Screening Based on Time Dependent DFT: ALDA. The functional for the self-energy replaces $W_{ref} \to W_{ALDA}$, where the TDDFT-screened interaction is given by

$$W_{ALDA}(1,2) = v(1,2) + \int d(34)v(1,3)\chi_{ALDA}(3,4)v(4,2) \tag{40}$$

$$\chi_{ALDA}^{-1}(1,2) = P_{KS}^{-1}(1,2) - v(1,2) - f_{XC}^{ALDA}(1,2) \tag{41}$$

with $f_{XC}^{ALDA}(1,2) = \delta v_{XC}^{ALDA}(\mathbf{r}_1)/\delta n(\mathbf{r}_2)\delta(t_1-t_2)$. In the case of a hybrid XC functional additionally exchange contributions weighted by a hybrid mixing parameter are also included. One in that case mixes TDDFT and TDHF in the calculation of the response function just as one mixes the DFT XC-functional and the HF exchange in the ground-state calculation.[63]

2.4.2. No Self-Consistency: G_0W_0-Approximation. In practice, one often terminates the iteration cycle for the GW_0-schemes already after the first step. There is no update in the self-energy, then, and one has $\Sigma^{(0)} = \Sigma[G_{in}]$ for the initial and final form of the self-energy matrix. As we have indicated already above, usually a good starting point for the iteration cycle is the KS-system,[64,65] hence $G_{in} = G_{KS}$ and

$$\Sigma^{(0)}(1,2) = iG_{KS}(1,2^+)W_{KS}(1,2^+) \tag{42}$$

Discussion. The last procedure in G_0W_0 can be rationalized by comparing to self-consistent GW in the following way. In GW we would aim at solving the following self-consistency problem

$$G = (G_H^{-1} - \Sigma[G])^{-1}$$

where the functional for the self-energy is specified by the simplifying GW-expression 28

$$\Sigma[G](1,2) = iG(1,2^+)W(1,2^+)$$

On the G_0W_0-level we stop the iteration cycle after the first step going from $G^{(0)} := G_{in} = G_{KS}$ to

$$G^{(1)} = (G_H^{-1} - \Sigma[G_{KS}])^{-1} = (G_{KS}^{-1} + V_{XC} - \Sigma[G_{KS}])^{-1}$$

dx.doi.org/10.1021/ct300648t | J. Chem. Theory Comput. 2013, 9, 232−246

In this procedure one essentially hopes that convergence in the cycle is fast enough, so that most of the *GW*-corrections are already contributed within the first iteration step. It should be clearly noticed that this approximation is neither controlled nor particularly systematic.

2.5. Linearized Quasi-Particle Equation. The leading order correction to the energies will be obtained, as usual, by working with the unperturbed wave functions. With this logic, also here we can employ 23 to evaluate 25 and thus get

$$\epsilon_n + \langle n|\Sigma[G_{KS}](z_n^{(1)}) - V_{xc}|n\rangle = z_n^{(1)}, \quad n = 1...N \tag{43}$$

In principle this equation now needs to be solved for the poles $z_n^{(1)}$. Notice, that one is working here with a zero iteration cycle only, i.e. G_0W_0, with respect to the self-energy, since Σ is calculated with the KS-Green's function and not updated. Hence, the self-consistent solution of eq 43, $z^{(1)}$, is not a pole of $\Sigma^{(0)}$. This is in contrast to the fully self-consistent solution, z_n, which is a pole of Σ.

This consideration suggests that faster convergence to the true *GW*-poles is achieved, if we linearize eq 43 in order to obtain an estimate. Written compactly we obtain

$$z_n^{(1)} = \epsilon_n + Z_n\langle n|\Sigma(\epsilon_n) - V_{xc}|n\rangle \tag{44}$$

which we take as the definition of $z^{(1)}$. Here, Z_n is given by

$$Z_n = \left[1 - \left\langle n\left|\frac{\partial\Sigma(E)}{\partial E}\right|_{E=\epsilon_n}\right|n\right\rangle\right]^{-1} \tag{45}$$

3. DYNAMICAL SCREENING

3.1. Density Response As an Eigenvalue Problem. In terms of the irreducible response function, P, the screened Coulomb interaction W is given by

$$W(\omega) = \varepsilon^{-1}(\omega)\cdot v = (1 - v\cdot P)^{-1}\cdot v \tag{46}$$

see Section 2.1, 6−10. Alternatively, we can construct W from the full (reducible) response function, $\chi = P + P\cdot v\cdot\chi$.

$$W(\omega) = v + v\cdot\chi(\omega)\cdot v \tag{47}$$

Since P enters W by an inversion, it can be advantageous from a numerical point of view to obtain W with χ directly, rather than via P. Indeed, consider the case where P^{-1} is easily obtained, while $(1 - Pv)^{-1}$ is hard to calculate. In this situation the inverse of χ is readily found:

$$\chi^{-1}(\omega) = P^{-1}(\omega) - v \tag{48}$$

The inversion of χ^{-1} can efficiently be done by investigating the eigensystem of this matrix. Namely, recall that like any other physical correlation function, $\chi(z)$ has a spectral representation. It specifies $\chi(z)$ in terms of its residues and poles in the complex plane. Since χ is a symmetric (complex) matrix and spans the same space as P, the two have the same number of poles, we may write $(z = \omega + i2\eta)$

$$\chi(\mathbf{r}, \mathbf{r}', \omega) = \sum_m \rho_m(\mathbf{r})\rho_m(\mathbf{r}')\left(\frac{1}{z - \Omega_m} - \frac{1}{z^* + \Omega_m}\right) \tag{49}$$

The pole positions, Ω_m, are the (charge neutral) excitation energies, and $\rho_m(\mathbf{r})$ denote the transition densities; m runs over all excitations, the product of the number of poles in the upper and the lower complex half planes of the Green's function, eq 31.[92]

The poles, Ω_m, can directly be obtained from analyzing the spectrum of the inverse χ^{-1}. Namely, we must have at the pole position, $z = \Omega_m$, of $\chi(z)$ a zero eigenvalue of $\chi^{-1}(z)$. So, we are looking for a combination of z and $\xi^{(m)}$, such that $\chi^{-1}(z)\xi^{(m)} = 0$ has a solution, explicitly

$$(P^{-1}(\Omega_m) - v)\xi^{(m)} = 0 \tag{50}$$

3.1.1. Derivation of the Generalized Eigenvalue Problem: RPA Equations. We next stipulated that like the full correlation function also the irreducible one has a spectral decomposition:

$$P(\mathbf{r}, \mathbf{r}', \omega) = \sum_n \Phi_n(\mathbf{r})\Phi_n(\mathbf{r}')\left(\frac{1}{z - \Omega_{rn}} - \frac{1}{z^* + \Omega_{rn}}\right) \tag{51}$$

In order to more easily facilitate the matrix inversion, we employ a trick and formally extend the matrix space we are working in. We rewrite P, χ, and $P\cdot v\cdot\chi$

$$P(\mathbf{r}, \mathbf{r}', \omega) = \sum_n (\Phi_n(\mathbf{r}), \Phi_n(\mathbf{r}))\Pi_{n,n}(\omega)\begin{pmatrix}\Phi_n(\mathbf{r}')\\ \Phi_n(\mathbf{r}')\end{pmatrix} \tag{52}$$

$$\chi(\mathbf{r}, \mathbf{r}', \omega) = \sum_{n,n'} (\Phi_n(\mathbf{r}), \Phi_n(\mathbf{r}))\Xi(\omega)_{n,n'}\begin{pmatrix}\Phi_{n'}(\mathbf{r}')\\ \Phi_{n'}(\mathbf{r}')\end{pmatrix} \tag{53}$$

$$[P\cdot v\cdot\chi](\mathbf{r}, \mathbf{r}', \omega) = \sum_{n,n',\bar{n}} (\Phi_n(\mathbf{r}), \Phi_n(\mathbf{r}))[\Pi_{n,n}(\omega)V_{n,\bar{n}}\Xi_{\bar{n},n'}(\omega)]\begin{pmatrix}\Phi_{n'}(\mathbf{r}')\\ \Phi_{n'}(\mathbf{r}')\end{pmatrix}$$

where

$$\Pi_{n,n'}(\omega) = \delta_{n,n'}\begin{pmatrix}(z - \Omega_{rn})^{-1} & 0\\ 0 & -(z^* + \Omega_{rn})^{-1}\end{pmatrix} \tag{54}$$

$$V_{n,n'} = v_{n,n'}\begin{pmatrix}1 & 1\\ 1 & 1\end{pmatrix} = \int d\bar{\mathbf{r}}d\bar{\mathbf{r}}'\begin{pmatrix}\Phi_n(\bar{\mathbf{r}})\\ \Phi_n(\bar{\mathbf{r}})\end{pmatrix}v(\bar{\mathbf{r}}, \bar{\mathbf{r}}')(\Phi_{n'}(\bar{\mathbf{r}}'), \Phi_{n'}(\bar{\mathbf{r}}')) \tag{55}$$

Fully analogous to their parent matrices P, v, and χ also the corresponding matrix kernels satisfy the following identity:

$$\Xi_{n,n'}(\omega) = \delta_{n,n'}\Pi_{n,n}(\omega) + \sum_{\bar{n}} \Pi_{n,n}(\omega)V_{n,\bar{n}}\Xi_{\bar{n},n'}(\omega) \tag{56}$$

In these objects the generalized eigenvalue problem 50 now reads

$$(\Pi^{-1}(\Omega_m) - V)\xi^{(m)} = 0 \tag{57}$$

or more explicitly

$$\sum_{\bar{n}}\left[\delta_{n,\bar{n}}\begin{pmatrix}\Omega_m - \Omega_{rn} & 0\\ 0 & -\Omega_m - \Omega_{rn}\end{pmatrix} - v_{n,\bar{n}}\begin{pmatrix}1 & 1\\ 1 & 1\end{pmatrix}\right]\begin{bmatrix}X_{\bar{n}}^{(m)}\\ Y_{\bar{n}}^{(m)}\end{bmatrix} = 0 \tag{58}$$

dx.doi.org/10.1021/ct300648t | J. Chem. Theory Comput. 2013, 9, 232−246

where the traditional notation $\xi^{(m)} = (X^{(m)}, Y^{(m)})$ has been introduced; in this notation

$$\rho_m(\mathbf{r}) = \sum_n (X_n^{(m)} + Y_n^{(m)})\Phi_n(\mathbf{r}) \tag{59}$$

To make eq 58 look more like a conventional eigenvalue problem, a notation is commonly introduced

$$\Delta = \begin{pmatrix} 1 & 0 \\ 0 & -1 \end{pmatrix} \tag{60}$$

so that

$$\Omega_m \Delta \begin{bmatrix} X_n^{(m)} \\ Y_n^{(m)} \end{bmatrix} = \sum_{\bar{n}} \left[\delta_{n,\bar{n}} \begin{pmatrix} \Omega_{rn} & 0 \\ 0 & \Omega_{rn} \end{pmatrix} + v_{n,\bar{n}} \begin{pmatrix} 1 & 1 \\ 1 & 1 \end{pmatrix} \right] \begin{bmatrix} X_{\bar{n}}^{(m)} \\ Y_{\bar{n}}^{(m)} \end{bmatrix} \tag{61}$$

Equation 61 is a density analogue of the quasi-particle equation, which we already derived from the Dyson equation for the Green's function. In a simple approximation one replaces the irreducible response P by the response of the noninteracting reference system. In this case Ω_{rm} denotes simply the energy cost for a bare (i.e., only coulomb screened) particle-hole excitation. If the single-particle reference system is Hartree−Fock, $P \to P_{\mathrm{HF}}$, this approximation is called RPA.

The RPA goes back to early work by D. Bohm and D. Pines in the field of nuclear physics.[66,67] Later it was introduced in the context of time dependent DFT by Casida[68] and used in the context of *GW* by Tiago and Chelikowsky.[37] In electronic structure literature the same approximation but using the KS-system as a reference, see the next section, is often also referred to as "RPA". In order to avoid confusion in terminology with the usage of RPA in standard condensed and nuclear matter text books, we refer to the conventional RPA as HF-RPA, while we will call the approximation based on the KS-system as KS-RPA, or "bare" KS-single particle response.

3.2. KS-Approximation for the Ground State Response. In this section we employ the approximation $P \to P_{\mathrm{KS}}$, with $(z = \omega + 2i\eta)$

$$P_{\mathrm{KS}}(\mathbf{r}, \mathbf{r}', \omega) = \sum_i \sum_a \psi_a^*(\mathbf{r})\psi_i(\mathbf{r})\psi_i^*(\mathbf{r}')\psi_a(\mathbf{r}') \times \left[\frac{1}{z - (\epsilon_a - \epsilon_i)} - \frac{1}{z^* + (\epsilon_a - \epsilon_i)} \right] \tag{62}$$

where as usual i runs over occupied states and a runs over unoccupied states.

The expression is readily derived from the basic definition of $P(1,2)$, 21, in terms of the causal Green's functions, 39. By comparing with eq 51 one concludes that ρ_m should be expanded in a basis of static spin orbital products

$$\rho_m(\mathbf{r}) = \sum_{i,a} (X_m + Y_m)_{i,a}\psi_i(\mathbf{r})\psi_a(\mathbf{r}) \tag{63}$$

where again $i,j,..$ label occupied states and $a,b,..$ label empty states. As explained in the previous section, the vectors $|X_m, Y_m\rangle$ are solutions of the non-Hermitian eigenvalue problem

$$(\Lambda - \Omega_m \Delta)|X_m, Y_m\rangle = 0 \tag{64}$$

under the orthonormality constraint

$$\langle X_m, Y_m|\Delta|X_{m'}, Y_{m'}\rangle = \delta_{m,m'} \tag{65}$$

and the operators

$$\Lambda = \begin{pmatrix} \mathrm{A} & \mathrm{B} \\ \mathrm{B} & \mathrm{A} \end{pmatrix}, \quad \Delta = \begin{pmatrix} 1 & 0 \\ 0 & -1 \end{pmatrix} \tag{66}$$

contain the orbital rotation Hessians

$$(\mathrm{A} + \mathrm{B})_{iajb} = (\epsilon_a - \epsilon_i)\delta_{ij}\delta_{ab} + 2\langle ij|ab\rangle \tag{67}$$

$$(\mathrm{A} - \mathrm{B})_{iajb} = (\epsilon_a - \epsilon_i)\delta_{ij}\delta_{ab} \tag{68}$$

with $\langle ij|ab\rangle = \int d\mathbf{r}d\mathbf{r}'\psi_i(\mathbf{r})\psi_j(\mathbf{r}')(1/(|\mathbf{r} - \mathbf{r}'|)\psi_a(\mathbf{r})\psi_b(\mathbf{r}')$.

3.3. TDDFT-Response. The exact TDDFT-representation of the irreducible density response is given after an inversion:

$$P^{-1}(\omega) = P_{\mathrm{KS}}^{-1}(\omega) - f_{\mathrm{XC}}(\omega) \tag{69}$$

The equation may be understood as an implicit definition for the TDDFT-kernel f_{XC}. The equivalent to eq 50 then reads

$$(P_{\mathrm{KS}}^{-1}(\Omega_m) - f_{\mathrm{XC}}(\Omega_m) - v)\xi^{(m)} = 0 \tag{70}$$

As already indicated above, 41, in the adiabatic LDA (ALDA) one replaces the TDDFT-kernel f_{XC} by the instantaneous ground state kernel in LDA approximation

$$f_{\mathrm{XC}}^{(\mathrm{ALDA})}(\mathbf{r}, \mathbf{r}', \omega) = \frac{\delta v_{\mathrm{XC}}^{(\mathrm{LDA})}[n](\mathbf{r})}{\delta n(\mathbf{r}')} \tag{71}$$

i.e., the functional derivative of the LDA XC-potential with respect to the ground-state density. As long as the XC-kernel does not pick up a frequency dependency, the numerical treatment of this equation follows the same computational lines as it does for standard LDA.

In TDDFT the calculation of the response function follows the same procedure as described in the previous section, with the difference that the f_{XC} is added to eq 67. In the case of a hybrid XC functional eqs 67 and 68 additionally contain exchange contributions weighted by the hybrid mixing parameter. More details can be found in the work of Furche and Ahlrichs.[63]

Remark: For G_0W_0 both theories, KS-GS and TDDFT in ALDA approximation, could be considered when calculating the density susceptibility. However, in the case where a self-consistent solution is to be achieved also with respect to χ, ALDA must be excluded from the second and all further iteration processes. ALDA cannot be used in the self-consistency cycle, because updating W_{KS} with the improved density does not eliminate the artifacts from the LDA-kernels.

4. CALCULATION OF THE MATRIX ELEMENTS OF Σ[G]

4.1. Self-Energies and Spectral Function. For the evaluation of the self-energy matrix elements we split the self-energy into an energy independent hermitian exchange and an energy dependent correlation part:

$$\Sigma(E) = \Sigma^{\mathrm{x}} + \Sigma^{\mathrm{c}}(E) \tag{72}$$

$$\Sigma^{x} = \frac{i}{2\pi}\int d\omega e^{-i\omega 0^{+}} G(E-\omega)v = -\int_{-\infty}^{\mu} dE' A(E'-\mu)v \tag{73}$$

$$\Sigma^{c}(E) = \frac{i}{2\pi}\int d\omega G(E-\omega)v\cdot\chi(\omega)\cdot v \tag{74}$$

In the second line the spectral representation of the (causal) Green's function, 15, has been used. Also the correlation part of the self-energy, Σ^{c}, can be formulated in terms of the spectral function ($z = \omega + 2i\eta$)

$$\begin{aligned}\Sigma^{c}(E) &= \frac{i}{2\pi}\int d\omega G(E-\omega)v\cdot\chi(\omega)\cdot v\\ &= \int_{-\infty}^{\infty} dE' A(E'-\mu)\sum_{m}(v\cdot\rho_m)(\rho_m\cdot v)\\ &\quad\times\frac{i}{2\pi}\int d\omega \frac{1}{E-E'-\omega+i\eta\,\mathrm{sgn}(E')}\\ &\quad\times\left(\frac{1}{z-\Omega_m}-\frac{1}{z^{*}+\Omega_m}\right)\\ &= \sum_{m}\int_{-\infty}^{\infty} dE' A(E'-\mu)(v\cdot\rho_m)(\rho_m\cdot v)\\ &\quad\times\frac{1}{E-E'-Z_m\,\mathrm{sgn}(E'-\mu)}\end{aligned} \tag{75}$$

where $Z_m = \Omega_m - 3i\eta$.

An equivalent expression for the matrix elements of the self-energy is also given by Hedin in his review paper of 1999.[9] Later it has been applied by Tiago et al. to molecular systems;[37] very recently the same approach has also been used by Bruneval.[56]

4.2. Matrix Elements of $\Sigma[G_{KS}]$. The bare KS-Green's function was given in eq 21. It exhibits the spectral function

$$A_{KS}(\mathbf{r},\mathbf{r}',E) = \sum_{n}\psi_n(\mathbf{r})\psi_n^{*}(\mathbf{r}')\delta(E-\epsilon_n) \tag{76}$$

Employing eq 73 and 75 the corresponding matrix elements of $\Sigma[G_{KS}]$ in the KS-basis are readily derived at energies matching the bare KS-values, $E = \epsilon_n$. These are the expressions needed for evaluating the linearized quasi-particle eq 44.

We have for the exchange part of the self-energy

$$\begin{aligned}\langle n|\Sigma^{x}|n'\rangle &= \left\langle n\left|-\int_{-\infty}^{\mu} dE' A_{KS}(E'-\mu)\cdot v\right|n'\right\rangle\\ &= -\sum_{\underline{n}}\left\langle\psi_n(\mathbf{r})\psi_{\underline{n}}(\mathbf{r}')\left|\int_{-\infty}^{\mu} dE'\delta(E'-\epsilon_{\underline{n}})v(\mathbf{r},\mathbf{r}')\right|\psi_{n'}(\mathbf{r}')\psi_{\underline{n}}(\mathbf{r})\right\rangle\\ &= -\sum_{\underline{n}}^{\mathrm{occ.}}(n\underline{n}|\underline{n}n') = -\sum_{i}(ni|in')\end{aligned} \tag{77}$$

where we have adopted the notation

$$(pq|rs) = \int d\mathbf{r}\int d\mathbf{r}' p(\mathbf{r})q(\mathbf{r})\frac{1}{|\mathbf{r}-\mathbf{r}'|}r(\mathbf{r}')s(\mathbf{r}')$$

The integrals in eq 77 are the usual exchange integrals as in HF. In a self-consistent treatment with respect to G (GW_0-level), using only this piece, i.e. not adding correlation, would hence restore exact exchange. The correlation part gives us

$$\begin{aligned}\langle n|\Sigma^{c}(E)|n'\rangle &= \sum_{\underline{n},\underline{n}'}\int_{-\infty}^{\infty} dE'\sum_{m}\langle\underline{n}|A_{KS}(E'-\mu)|\underline{n}'\rangle\\ &\quad\times\langle\underline{n}'|\langle n|(v\cdot\rho_m)(\rho_m\cdot v)|n'\rangle|\underline{n}\rangle\\ &\quad\times\frac{1}{E-E'-Z_m\,\mathrm{sgn}(E'-\mu)}\\ &= \sum_{\underline{n},\underline{n}'}\int_{-\infty}^{\infty} dE'\sum_{m}\delta_{\underline{n},\underline{n}'}\delta(E'-\mu-\epsilon_{\underline{n}}+\mu)\\ &\quad\times\langle\underline{n}'|(v\cdot\rho_m)|n'\rangle\langle n|(\rho_m\cdot v)|\underline{n}\rangle\\ &\quad\times\frac{1}{E-E'-Z_m\,\mathrm{sgn}(E'-\mu)}\\ &= \sum_{m}\sum_{\underline{n}}(\underline{n}n|\rho_m)(\rho_m|n'\underline{n})\\ &\quad\times\frac{1}{E-\epsilon_{\underline{n}}-Z_m\,\mathrm{sgn}(\epsilon_{\underline{n}}-\mu)}\end{aligned} \tag{78}$$

The on-shell diagonal matrix elements simplify:

$$\langle n|\Sigma^{c}(\epsilon_n)|n\rangle = \sum_{m}\sum_{\underline{n}}\frac{|(\underline{n}n|\rho_m)|^2}{\epsilon_n-\epsilon_{\underline{n}}-Z_m\,\mathrm{sgn}(\epsilon_{\underline{n}}-\mu)} \tag{79}$$

4.3. Energy Shifts of Quasi-Particles on the G_0W_0-Level. Eventually, we will be mainly interested in the interaction induced shift of the quasi-particle energies, i.e., in $\epsilon_n^{(1)} = \mathrm{Re}z_n^{(1)}$. It is given by the real part of the linearized quasi-particle equation, 44,

$$\epsilon_n^{(1)} = \epsilon_n + \mathrm{Re}Z_n[\langle n|\Sigma^{x}|n\rangle + \mathrm{Re}(\langle n|\Sigma^{c}(\epsilon_n)|n\rangle) - \langle n|V_{xc}|n\rangle] \tag{80}$$

$$\mathrm{Re}Z_n = \left[1 - \mathrm{Re}\left(\left\langle n\left|\frac{d\Sigma^{c}(E)}{dE}\right|_{\epsilon_n}\right|n\right\rangle\right)\right]^{-1} \tag{81}$$

The real part of the diagonal matrix elements of Σ have exchange contribution given by

$$\langle n|\Sigma^{x}|n\rangle = -\sum_{i}(ni|in) \tag{82}$$

while for the correlation contribution we have ($3\eta \to \tilde{\eta}$)

$$\begin{aligned}&\mathrm{Re}(\langle n|\Sigma^{c}(\epsilon_n)|n\rangle)\\ &= \sum_{m}\left[\sum_{i}|(in|\rho_m)|^2\frac{\epsilon_n-\epsilon_i+\Omega_m}{(\epsilon_n-\epsilon_i+\Omega_m)^2+\tilde{\eta}^2}\right.\\ &\quad\left.+\sum_{a}|(an|\rho_m)|^2\frac{\epsilon_n-\epsilon_a-\Omega_m}{(\epsilon_n-\epsilon_a-\Omega_m)^2+\tilde{\eta}^2}\right]\end{aligned} \tag{83}$$

dx.doi.org/10.1021/ct300648t | J. Chem. Theory Comput. 2013, 9, 232−246

where as before m runs over all density excitations. The real part of the diagonal matrix elements of the energy derivative of the self-energy:

$$\mathrm{Re}\left(\left\langle n\left|\frac{d\Sigma^c(E)}{dE}\right|_{\epsilon_n}\right|n\right\rangle\right) = \sum_m\left[\sum_i |(in|\rho_m)|^2\frac{\tilde{\eta}^2-(\epsilon_n-\epsilon_i+\Omega_m)^2}{[(\epsilon_n-\epsilon_i+\Omega_m)^2+\tilde{\eta}^2]^2} + \sum_a |(an|\rho_m)|^2\frac{\tilde{\eta}^2-(\epsilon_n-\epsilon_a-\Omega_m)^2}{[(\epsilon_n-\epsilon_a-\Omega_m)^2+\tilde{\eta}^2]^2}\right] \quad (84)$$

4.4. Details of the Implementation. Calculating the G_0W_0-quasi-particle energies can now be performed in three steps. First a ground state DFT-calculation is performed providing the KS-orbitals and energies $\psi^{(0)}$ and $\epsilon^{(0)}$. It is followed by a TDDFT-calculation providing the response of the system in terms of the expansion coefficients $(X+Y)^m_{ia}$ of the excitation densities ρ_m. In the final step the G_0W_0-quasi-particle energies are calculated according to eqs 80 to 84. The basic quantities needed in these equations are $\langle n|V^{xc}|n\rangle$, $\Sigma_i(ni|in)$, and $(\underline{n}n|\rho_m)$, and we will now comment on how to obtain them making optimal use of code usually already existing in any quantum chemistry package. Our implementation was made in the TURBOMOLE package.

Evaluation of the matrix elements of the exchange correlation potential $\langle n|V^{xc}|n\rangle$ obviously also occurs in the DFT-calculation itself. They can therefore be stored after the DFT-calculation has been finished or be recalculated by calling the existing routine again. The second quantity, the exchange contribution to the self-energy $\Sigma_i(ni|in)$, is the same as the exchange appearing in a Hartree−Fock calculation. In this case however, it is evaluated at KS-orbitals instead of HF-orbitals. Hence, given that algorithms for HF calculations or hybrid functionals are available, again already existing routines can be used to obtain the required quantity. Finally, a routine to calculate the matrix elements $(\underline{n}n|\rho_m)$, needed for the correlation part of the self-energy, can be built from parts of code used in the TDDFT-calculation. In solving the eigenvalue problem described in Section 6.2 and Section 6.3 matrix elements of the same type occur. The remaining task to be implemented is the evaluation of the sums in eq 83 and 84.

From the three quantities described above the most time-consuming to calculate is $(\underline{n}n|\rho_m)$. We elaborate on it is calculation to understand the computational scaling and investigate possible improvements. Expanding the orbitals ψ_n in a series of local basis-functions ϕ_ν, in our case Gaussian orbitals, $\psi_n(\mathbf{r}) = \Sigma_\nu c_{\nu n}\phi_\nu(\mathbf{r})$ yields

$$(\underline{n}n|\rho_m) = \sum_{ia}(\underline{n}n|ia)(X+Y)^m_{ia} = \sum_{\mu\nu\kappa\lambda} c_{\underline{n}\nu}c_{n\mu}(\nu\mu|\kappa\lambda)(X+Y)^m_{\kappa\lambda} \quad (85)$$

$$(X+Y)^m_{\kappa\lambda} = \sum_{ia} c_{\kappa i}(X+Y)^m_{ia}c_{a\lambda} \quad (86)$$

The coefficients of the excitation vectors $(X+Y)^m_{ia}$, which are the result of the preceding TDDFT-calculation, are available on file. They are read in blocks of excitations and transformed to the Gaussian basis, $(X+Y)^m_{ia} \rightarrow (X+Y)^m_{\kappa\lambda}$, eq 86. In the next step the integrals $(\nu\mu|\kappa\lambda)$ are calculated and directly contracted with $(X+Y)^m_{\kappa\lambda}$ and transformed back to the basis of molecular orbitals, eq 85. The block size and thus the number of repeated evaluations of the integrals is determined by the amount of available core memory, which is given as an input parameter.

For each excitation the step in eq 85 formally scales like N^4_{BF} (N_{BF} the numbers of basis functions). However, when μ and ν are based at atoms far apart the integral $(\mu\nu|\kappa\lambda)$ vanishes. By using an index array the number of integrals that need to be evaluated can be reduced, and the asymptotic scaling for large systems becomes N^2_{BF}.

The prefactor of the step in eq 85 can be reduced by a factor of ca. 10 employing density fitting (also called the "resolution of the identity", RI).[69,70] In this approach the products of basis functions are approximated by a series of so-called auxiliary basis functions $P(\mathbf{r})$ and eq 85 becomes

$$\sum_{\kappa\lambda}(\nu\mu|\kappa\lambda)_{RI}(X+Y)^m_{\kappa\lambda} = \sum_{\kappa\lambda PQ}(\nu\mu|P)(P|Q)^{-1}(Q|\kappa\lambda)(X+Y)^m_{\kappa\lambda} \quad (87)$$

The integrals $(Q|\kappa\lambda)$ are computed and directly contracted with all excitation vectors $(X+Y)^m_{\kappa\lambda}$ of the current block of excitations. The resulting vector is multiplied with the precomputed matrix $(P|Q)^{-1}$ and the result with $(\nu\mu|P)$. The formal scaling behavior then is $N^3_{BF}N_{occ}N_{virt}$, the asymptotic the same as without RI. Further acceleration of this time-determining step may be achieved by neglecting weakly contributing excitation vectors. Moreover, this step can be parallelized very efficiently.

The calculation of level shifts in eq 83 requires the pre-calculation of - presently - all excitation vectors $(X+Y)^m$. The calculation of the excitation vectors is an iterative procedure where in each iteration, tasks very similar to the calculation of $(\underline{n}n|\rho_m)$ have to be performed. In addition, in each iteration step the respective exchange-correlation part needs to be calculated, see Section 3.3. The calculation of the excitation vectors is therefore much more time-consuming than the calculation of the quasi-particle energies. Thus, in order to achieve improvement on the computational effort, further developments have to be focused on neglecting or approximate treating of weakly contributing excitations. Nevertheless, already with the present implementation (no parallelization and without exploiting the molecular symmetry) molecules as large as naphthacene can be treated with a basis flexibly enough to obtain results converged within 0.2 eV within 5 days.

5. TOWARD BENCHMARK RESULTS

To test our implementation and give first benchmarks we performed calculations on a test set of 27 typical molecules ranging from H_2 to naphthacene, see Figure 1. The rest of the paper will refer to this set as GW27. For most molecules the structures are taken from the database supplied with the TURBOMOLE distribution. For certain dimers and the higher aromatic molecules anthracene and naphthacene, which are not supplied there, we optimized the structures employing the same optimization conditions that were used to determine the structures in the database. The G_0W_0-results presented in this section have been calculated starting from DFT using the PBE functional and applying the TDDFT-screening, see Section 3.3. In the calculation of the matrix elements of the correlation part of the self-energy, eq 83 and 84, η was chooses so small that the values were converged within 0.01 eV. In most cases η = 1 meV was used. In all calculations the RI approximation has been applied,[71] the effect of this, and other, approximations is studied in the next section.

dx.doi.org/10.1021/ct300648t | J. Chem. Theory Comput. 2013, 9, 232−246

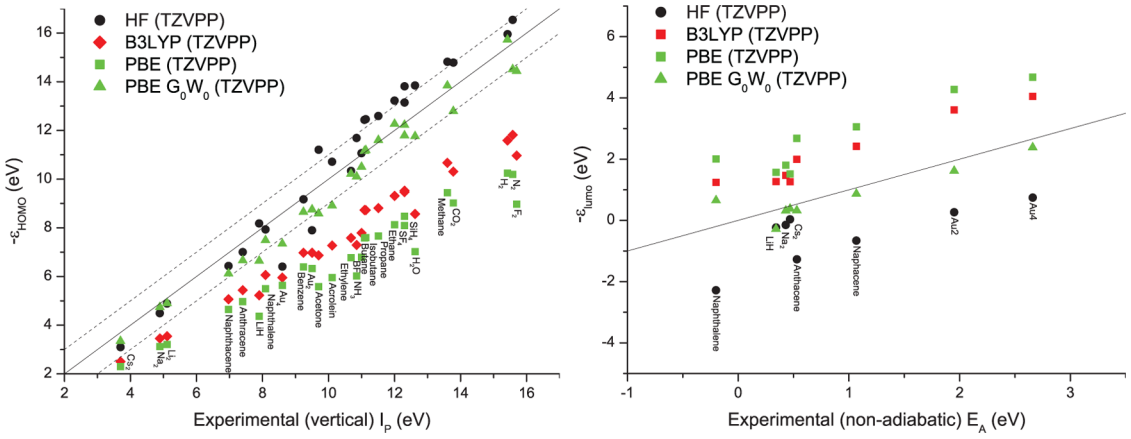

Figure 1. Comparison of experimental (horizontal axis) with theoretical (vertical axis) ionization energies, left, and electron affinities, right. Results from HF-calculation, DFT with PBE and B3LYP functional, and G_0W_0 (@PBE using TDDFT-response) calculations are shown. In all calculations the TZVPP basis set has been used.

In order to demonstrate the accuracy of our G_0W_0-procedure, one would ideally compare to the results of more consistent approaches, e.g. GW_0, fully self-consistent GW or, optimally, the exact solution of Hedin's equations. Such more advanced results are not available, however, for our entire test set of molecules.[93] Therefore, we resort to a common work-around comparing to experimental values.

5.1. Ionization Potentials for the Test Set GW27. Our first test observables will be the first, vertical ionization energy/potential (I_P) and electron affinity (E_A). We can extract them directly from the Green's function because its quasi-particle spectrum, by definition, corresponds to minus the (vertical, primary) I_P for the occupied orbitals, $\varepsilon_i = -I_{Pi}$, and to minus the (nonadiabatic) electron affinities for the unoccupied (binding) orbitals, $\varepsilon_a = -E_{Aa}$. In the assessment of the G_0W_0-results we will include a comparison to I_P's and E_A's obtained from HF and DFT. It will provide a rough quantitative measure for the improvement that can be obtained from G_0W_0 with respect to well-known procedures. In HF we have direct access to both quantities via Koopmans' theorem. In DFT the HOMO energy level can be associated with minus the first ionization energy.[72−74] We will also use the DFT LUMO energy levels as E_A's in the comparison. In doing this we neglect the derivative discontinuity.

The DFT-results with the semilocal PBE XC-functional[75−78] have an I_P undershooting the experimental value by roughly 35%, see Figure 1. This is a typical well-known artifact of local approximations in LDA- or GGA-type XC-functionals.[15] Most notably, the approximate treatment of exchange induces a spurious interaction of electrons with their own charge distribution, which artificially enhances, e.g., the HOMO-energies. The effect is most pronounced for systems with localized charge densities, i.e. small molecules and transition metals.

On HF level exchange is treated exactly, so the associated I_P exceeds the DFT-estimate considerably. Quantum fluctuations of the effective medium seen by an electron are completely neglected in the HF approximation. These correlation effects are much smaller than the "self-interaction" as long as relatively small molecules are concerned; roughly an order of magnitude. Correlation tends to make ionization easier, the neglect of it by HF hence typically causes an overestimation of the I_P, see Figure 1.

The hybrid functional B3LYP[75,76,79−82] mixes a fraction of Fock exchange into the DFT-functional. In this way it reduces the self-interaction of the orbitals, at the cost of becoming nonlocal and introducing an extra parameter, a_0, that interpolates between DFT and HF. The value of the parameter, $a_0 = 0.2$, was determined empirically by optimizing with respect to the reproduction of the atomic structure for a test set of molecules.[82] As can be seen from Figure 1, the increase of I_P starting from the DFT- toward the HF-estimate is roughly reflecting the admixture-parameter: $a_0 \approx (I_P^{B3LYP} - I_P^{DFT})/(I_P^{HF} - I_P^{DFT})$. (Here we neglect that B3LYP also contains correlation contributions, i.e., B3LYP at $a_0 = 1$ does not correspond to pure HF.)

So far we have reproduced a well-known hierarchy of functional approximations. The self-consistent GW-approach subtracts the XC-part of the DFT-functional and adds exact exchange instead. Already on the G_0W_0-level, much of the spurious self-interaction of KS-particles is removed in this way. This is the main reason why the G_0W_0-I_P are seen to increase substantially toward the HF-estimates in Figure 1. In addition, GW also provides a part of the correlation contributions that make the difference between HF- and the true I_P. As a consequence of both observations, the G_0W_0 HOMO quasi-particle energies of the GW27 molecules have a root-mean-square deviation from the vertical first ionization potential of only 0.47 eV. Moreover, they do not show any systematic under- or overestimation with respect to the absolute value. This compares to the systematic under estimation of DFT by 35% (absolute deviations ranging from 1 to 5 eV) and overestimation of HF by 7%. For the electron affinities the picture is similar. The G_0W_0 LUMO quasi-particle energies of the GW27 molecules have a root-mean-square deviation from the electron affinities of 0.65 eV, compared to 1.75 eV for DFT (PBE) and 1.39 eV for HF.

Summarizing, we find that both the absolute values of the HOMO and LUMO energies and the trend of the HOMO energies (slope in Figure 1 of the HOMO energies with increasing I_P) of the four approaches is best reproduced by the GW-approach. The good description of the trend ensures that relative energy levels are predicted accurately. This is very important for the correct description of the charge transfer that occurs if different molecules are combined to a larger entity. This encouraging feature is a particular aspect of GW that does not exist with DFT or HF.

5.2. Higher Ionization Energies of Simple Molecules: H_2O, N_2, C_6H_6. In the following sections we discuss in detail three typical molecules, H_2O, the nitrogen dimer N_2, and benzene C_6H_6, to assess the accuracy of the G_0W_0-approximation for higher ionization energies. Again we compare to HF and DFT with hybrid and nonhybrid functionals. Additionally, we include in the comparison the I_P's obtained from DFT total energies

dx.doi.org/10.1021/ct300648t | J. Chem. Theory Comput. 2013, 9, 232−246

by applying a self-consistent field (ΔSCF) method. In this approach the first ionization energies are calculated as total energy differences

$$I_P = E(N-1) - E(N)$$

where $E(N)$ is the total energy of the N electron system. The ΔSCF method is in principle exact and known in many cases to be very accurate for approximate functionals, mainly because of error cancellation. This method can always be used to obtain the first ionization energy.

To use the ΔSCF method to calculate also the higher ionization energies requires the calculation of $E(N-1)$ for an excited state. Since DFT is only valid for the ground state, it can formally not be used to obtain the energies of these states. Using a special recipe we can however often obtain an approximate value. In this approach the initial guess for the orbitals, from which the DFT self-consistency cycle is started, is created with a hole in the spectrum. If this initial point is close to a local self-consistent minimum and the optimization routine does not take too large steps, i.e., it stays in the valley of the local minimum, the energy of an excited $N-1$ electron state can be found. From the energies of these states other primary ionization energies can be calculated.

5.2.1. H_2O. Although being a small molecule the strongly polar covalent character of bonding gives H_2O a nontrivial electronic structure. Its ubiquitous appearance in almost every branch of chemistry makes it an important benchmark system for any computational approach. For the first three I_P's we get an agreement of G_0W_0 with both the experimental and the ΔSCF values that is an order of magnitude better than the average level spacing, see Figure 2 (left). For the fourth level G_0W_0 overestimates by 2 eV, where ΔSCF overestimates by 1 eV. This implies that in this case the KS-orbital is a bad approximation for the true quasi-particle state, which is also reflected in the bad description of the single occupation of this orbital in the ΔSCF calculation.

5.2.2. N_2. The nitrogen dimer is another interesting example. Already in the seventies it was observed that the order of the HF-levels has the first two levels reversed with respect to what is known from experiments (breakdown of Koopmans' theorem), see Figure 2 (right).[83] This reversal is known to originate from the large differences in correlation energy of the corresponding orbitals. The HOMO, a rather compact σ molecular orbital, has a much higher correlation energy than the HOMO-1 (and HOMO-2), extended π, molecular orbitals. The difference in this case is so large, 0.9 eV, that the orbital order is reversed if the correlation contributions are neglected, as is the case in HF; both DFT and *GW* show a proper ordering of the levels.

In butane and larger alkanes a different situation occurs, where now the DFT-ordering is wrong as well. In butane when treated with approximate DFT-functionals (both B3LYP and PBE) the HOMO (a_g) and HOMO-1 (b_g) levels are interchanged, see ref 84 and references therein. It has been shown before that by including diagrams in the self-energy up to third order with respect to the HF-reference (ADC(3)), the poles of the Green's function do get the right ordering.[85] The G_0W_0-approximation for the self-energy also includes such important diagrams and hence also leads to the proper ordering of the levels.

5.2.3. Benzene. We conclude this section with the most studied test molecule, benzene. The ten lowest primary ionization potentials are well determined experimentally. Over the whole range of valence states we observe a good description by the G_0W_0-method, where HF increasingly underestimates and DFT increasingly overestimates with increasing energy, see Figure 3. In particular, the deviations of the G_0W_0-results from the experimental values are smaller than the overall level spacing. We also observe that the ΔSCF method has increased difficulties for this system since for the lowest two I_P's no metastable self-consistent solution with a hole in these levels could be obtained. It does however still make a significant improvement with respect to the bare KS-values. For the first eight I_P's the ΔSCF values are shifted with respect to the KS by about 3 eV toward the experimental values. After this shift there is a residual deviation of the ΔSCF from the experimental values. This deviation mainly follows the KS-energies, hence, both methods suffer from the approximate XC-functional in a similar way.[94] The G_0W_0-results, although being based on the DFT-results, do not follow this trend.

6. CONVERGENCE TESTS

In this section we perform two types of convergence tests and a comparison to another implementation of the G_0W_0-method. In the first subsection, Section 6.1, we show how well our G_0W_0-I_P's are converged for the set of test molecules with respect to the size of the Gaussian basis set. In particular we show that the results do converge and that an extrapolation can be used to estimate a complete basis set limit. For solids the dependence of G_0W_0-results on the exchange-correlation functional of the underlying DFT-calculation has been studied intensively.[87,88] In Section 6.2

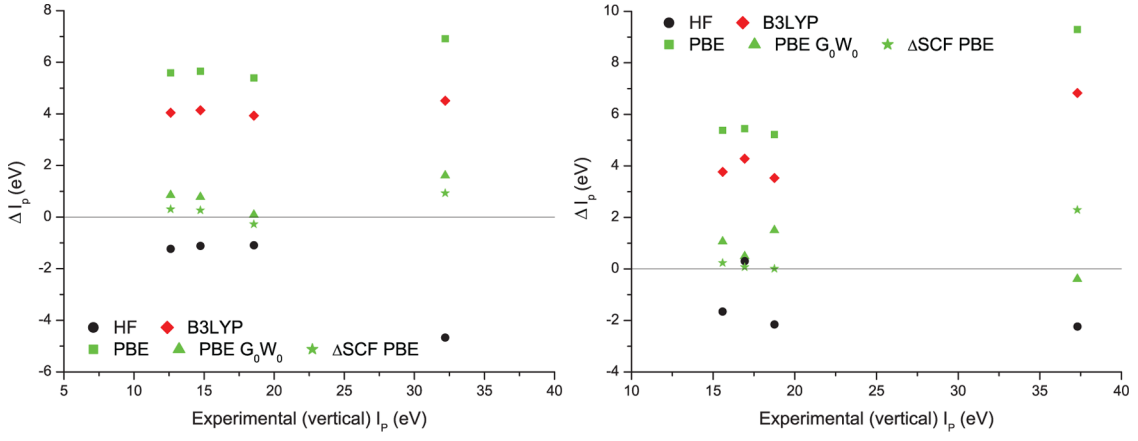

Figure 2. Deviation of the quasi-particle spectrum, HF- and KS-single particle energies of H_2O (left) and N_2 (right) from the experimental vertical ionization potentials (I_P), plotted over this value I_P. Calculations performed with TZVPP-basis set.

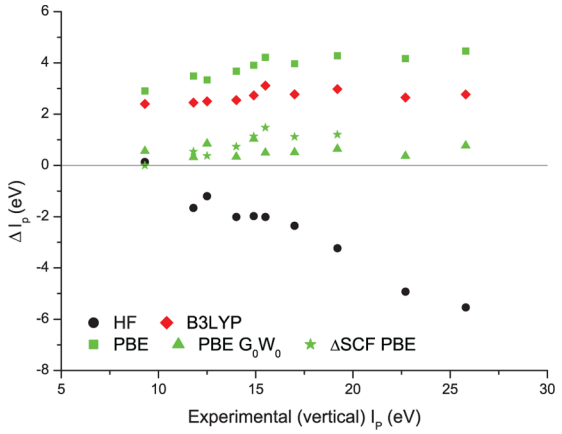

Figure 3. Data similar to Figure 2 for benzene. It is seen once again that the performances of ΔSCF and G_0W_0 are roughly comparable for the lower lying (six) vertical potentials, while HF and DFT fail to capture the experimental trend.

we demonstrate that already on the G_0W_0-level the dependency of the I_P's of the test set molecules on the XC-functional is strongly reduced. In the last subsection a comparison with results obtained by another *GW*-implementation is performed. It will be seen that the two implementations give quantitatively similar results.

The G_0W_0-results presented here always contain a full sum over the occupied and unoccupied orbitals, and over the excitations, the sums over *i*, *a*, and *m* in eq 83 respectively. The effect of the RI approximation was tested for all systems and found to be smaller than 0.1 eV in all cases, in most cases smaller that 0.02 eV, indicating that the quality of the auxiliary basis functions[71] is sufficient for our G_0W_0-calculations. Increasing the size of the grid for the quadrature of exchange-correlation terms beyond the standard size has effects below 1 meV.

6.1. Basis Sets. We start the study of the basis set dependence of the G_0W_0-I_P's by comparing, for three small molecules, H_2O, N_2, and CH_4, the results obtained using both the def2-SVP, TZVP, TZVPP, QZVP and the cc-pVXZ, X = D,T,Q,5, basis set series, see Figure 4 left.[71] The results can be extrapolated when plotted against the inverse of the number of basis functions for both series of basis sets. For the def2 basis sets the TZVP, TZVPP, QZVP results can be extrapolated by a linear fit for the three molecules. For CH_4 and N_2 the SVP result also falls within this linear fit. For H_2O the convergence is so rapid, that the deviation between the results for the two largest basis sets is already negligible.

Based on the observation for the three small molecules above, we extrapolate the def2 results for the entire GW27 test set in the same way. We extrapolate the results, from the basis sets for which KS-orbital energy and exchange part of the self-energy are converged, against the inverse of the number of basis-functions by a linear fit. The value of this fit at zero is taken as an estimate for the complete basis set (CBS) limit. The results of the four basis sets and the estimated CBS limit are shown in Figure 4 right.

The SVP results deviate up to 0.65 eV from the CBS limits. The largest deviations (≥0.4 eV) are seen for a group of molecules (from left to right LiH, CO_2, H_2O, NH_3, SF_4, acetone, acrolein) with strong polar covalent bonds where the SVP basis set clearly is not able to describe the bonding very accurately. We observe that for these molecules already the DFT-HOMO energy levels show a similar deviation when calculated with the SVP basis set. The SVP results were for these molecules excluded from the linear fit to obtain the CBS limit.

The TZVP basis set already brings the deviation below ~0.3 eV. Especially the group deviating strongly at the SVP basis is not standing out any more. Adding another set of polarization functions (applying the TZVPP basis set) brings the deviation from CBS limit within 0.2 eV for most molecules.[95] The dominating effect of the increase in basis functions above TZVP comes not anymore from a correction to the binding orbitals but from an increased number of virtual orbitals, changing only the correlation part of the *GW*-self-energy.

From the results presented in this section we conclude that the TZVPP basis set is a reasonable compromise between numerical accuracy and computational effort for G_0W_0-calculations on molecules. Therefore, the TZVPP basis set will be used for the comparison between different DFT XC-functionals in the next section. We mention that for the other functionals a comparison between the SVP and TZVPP basis gives a similar picture as has been shown here for the PBE functional.

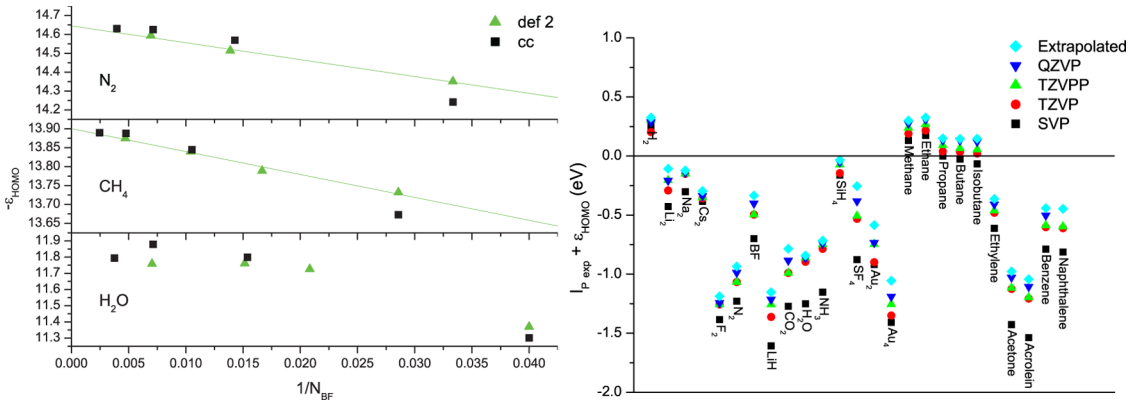

Figure 4. Convergence test of the G_0W_0-ionization potential with respect to the size of the basis set (using the def2-SVP, TZVP, TZVPP, QZVP basis sets). Left: The G_0W_0-IP's of N_2, CH_4, and H_2O plotted against the reciprocal of the number of basis functions. The lines represent the linear fit to the def2 results used to estimate a complete basis set limit. For H_2O results converge quickly; the data for the two largest basis set have deviations already less than 5 meV. For comparison also the results obtained using cc-pV[DTQ5]Z basis sets are plotted. Right: The G_0W_0-IP's obtained using the four basis sets together with the estimated complete basis set limit results. This plotting highlights the fact that the basis set convergency is relatively homogeneous over our test set GW27.

dx.doi.org/10.1021/ct300648t | J. Chem. Theory Comput. 2013, 9, 232−246

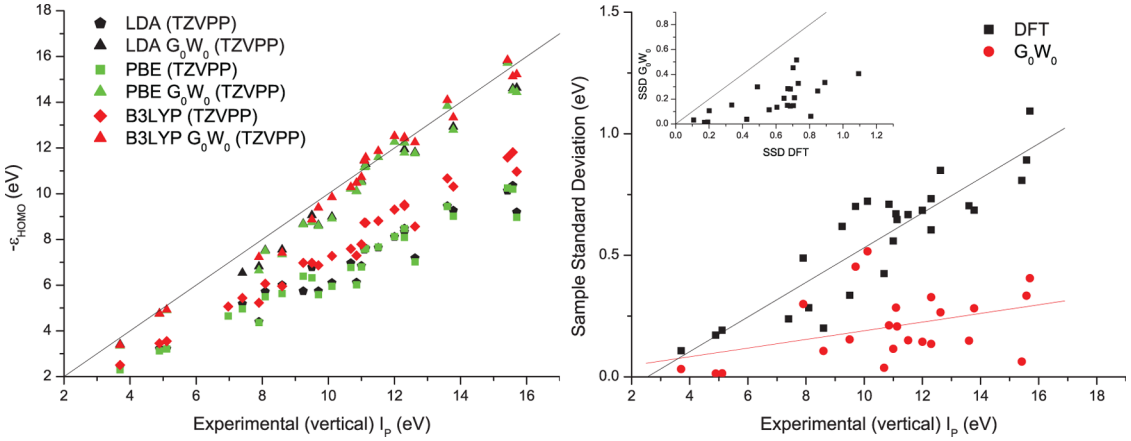

Figure 5. Left: Sensitivity of the G_0W_0-quasi-particle energies on the choice of the XC-functional underlying the parent DFT-calculation. Calculations are performed with the TZVPP basis set. Left: Root Mean Square Deviations of the DFT and G_0W_0-quasi-particle energies. Right: Sample standard deviation (SSD) of the G_0W_0 and DFT HOMO energies using different functionals, LDA, PBE, and B3LYP, plotted against the experimental I_P's. The inset shows the SSDs of G_0W_0 data plotted against those of the corresponding DFT-data.

6.2. Sensitivity to XC-Functionals on the G_0W_0-Level. In fully self-consistent *GW* the results do in general not depend on the DFT-functional used to calculate the initial Green's and response function. Interrupting the self-consistency-cycle already after the first iteration, as we do in the G_0W_0-approximation, the full initial spread is reduced, but some residual dependency of the calculated observables on the choice of the initial XC-functional prevails. Figure 5 illustrates this.[96]

As can be seen in Figure 5, right, the spread in KS-energies obtained with LDA, PBE, or hybrid functionals considerably exceeds the corresponding one of G_0W_0-quasi-particle energies. The *GW*-results tend to be in most cases within 1 eV of the experimental value and mostly are even closer to each other. This suggests that the G_0W_0 is already close to the self-consistent result.

In some cases the G_0W_0-results depend significantly on the DFT-functional. A clear example is LiH (I_P = 7.9), and to a lesser extent, the hydrocarbons with OH groups (I_P = 9.7 and 10.11) and H_2O (I_P = 12.6). The strong polarization arising from the large difference in electron affinity seems to be a regime where the hybrid and nonhybrid functionals lead to significantly different orbitals. This is clear in the case of LiH where the PBE HOMO-orbital is 50% more delocalized than the B3LYP HOMO-orbital.

The comparison shows that in many cases one can suffice by using a (semi) local XC-functional for the underlying DFT-calculation. This clearly comes with a computational advantage since in that no exchange integrals have to be evaluated in the calculation of the response function. One has to be careful however if strongly polar covalent bonds are present.

6.3. Comparison with Another *GW*-Approach. Using the same atomic structures, calculations were also performed with the FHI-aims code.[52,57] The general approach in FHI-aims differs from that used in TURBOMOLE: in FHI-aims the basis-functions are strictly local and numerical, in contrast to the contracted Gaussian orbitals used in TURBOMOLE. More importantly, the G_0W_0-implementation in FHI-aims uses the imaginary time formalism with analytic continuation to perform numerical energy integrations, while in our approach these can be performed analytically. The results from both codes should converge to the same values for physical observables with respect to the used basis functions, accuracy of the analytic continuation and energy integration grid. The comparison is therefore useful to test both approaches and implementations. The calculations with FHI-aims are preformed using "really tight Tier 3" settings and a Gaussian occupation of 10 meV width.[97]

Besides the mentioned differences the G_0W_0-implementation in FHI-aims uses KS-RPA instead of TDDFT-response and iteratively solves the quasi-particle eq 43, where we use the linearized quasi-particle equation, 44. To make a proper comparison we also implemented an iterative solving scheme and switch to KS-RPA response, see Section 3.2 and Section 3.3. Solving eq 43 in general increases the HOMO levels by up to 0.1 eV (see Figure 6). This can be seen as a correction to a slight overshooting of results obtained by using the linearized quasi-particle equation, 44. Switching from TDDFT to KS-RPA response, on the other hand, decreases the HOMO energies, also up to 0.1 eV. This difference is expected because of a smaller screening in KS-RPA response and hence, in absolute value, smaller Σ^c, less negative, matrix elements.

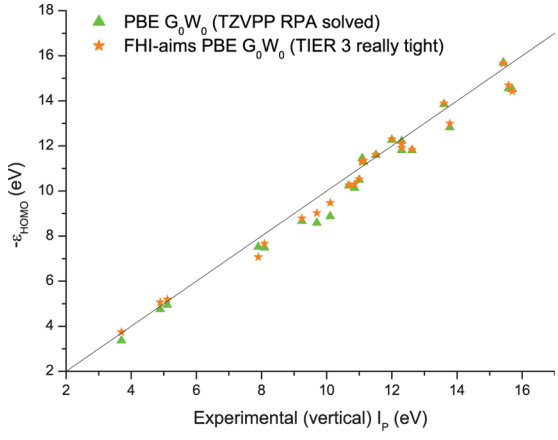

Figure 6. The G_0W_0 HOMO energy levels, using two implementations of G_0W_0 compared to experimental vertical ionization potentials. Compared are the basis sets TZVPP and Tier 3 basis set. One set of calculations is performed using the implementation described in this manuscript, one using the FHI-aims code. The values presented here all use an iterative solving of the quasi-particle eq 43 and RPA response.

The overall agreement between the results from the two codes is encouraging. Some discrepancies remain with FHI-aims that we mainly ascribe to differences in basis sets used. A more

detailed comparison with FHI-aims, using identical basis sets and a much larger set of molecules, is currently being prepared in collaboration.

7. CONCLUSIONS

In this paper we have reviewed the *GW*-approach and described a way how to build its most used approximation, G_0W_0, efficiently into a quantum chemistry package. The special feature of the design we followed is the use of spectral representations for the response and Green's function. This enables an analytic evaluation of energy integrals and derivatives. In particular the matrix elements of the self-energy Σ can be expressed directly in terms of two electron integrals, which are often readily available in standard packages. Therefore, the resulting expressions can be implemented efficiently in any generic quantum chemistry code. In our implementation in TURBOMOLE the use of a basis set of contracted Gaussians and the application of the RI method greatly improve the computational efficiency. We showed that G_0W_0 implemented in this way has the potential to treat medium sized molecules at moderate computational cost.

A second advantage of the approach followed here is that the analytical evaluation of the energy integrals avoids the use of further approximations. It avoids the uncertainties that may arise of the plasmon-pole models often used and prevents additional computational parameters needed in numerical frequency integration methods.

Both the vertical primary ionization potentials and the electron affinities of a test set of molecules have been calculated. In agreement with previous studies the results were shown to be mostly within 0.6 eV of the experimental values, at most, in the GW27 test set, deviating by 1.2 eV.[37,38,42,52] Moreover, the deviations do not grow with the absolute value of the I_P or E_A. This strongly contrasts DFT and HF that both show an increased deviation with increasing I_P.

The main approximation in solving numerically the G_0W_0-equations lies in the finiteness of the basis set. The dependence on the basis set was investigated by comparing the hierarchical series of def2-SVP, TZVP, TZVPP, and QZVP basis sets.[71] For a set of small molecules we tested convergence by including additionally correlation consistent double to quintuple zeta basis functions (cc-pVDZ to cc-pV5Z). This showed a convergence that can be extrapolated to the complete basis set limit to which the TZVPP results are converged within 0.25 eV. From the results obtained using the different basis sets we deduce that the TZVPP basis set is a practical compromise between accuracy and computational effort.

By comparing the G_0W_0-results obtained using different functionals for the underlying DFT-calculation we investigated the residual functional dependence. It was shown that the spread in the G_0W_0-I_P's of the GW27 test set is in general a factor of two to five times smaller than the DFT ones. Moreover, where the spread in the DFT-results increases with increasing absolute value of the I_P, the spread in the G_0W_0-results stays more or less small and constant. This observation gives hope that the self-consistency loops contained in the full *GW*-calculation may converge under generic conditions very rapidly, so that the G_0W_0-results may exhibit deviations from fully converged results that can be neglected for many practical purposes.

■ ASSOCIATED CONTENT

Supporting Information

Full details of the used atomic structures and tables containing the calculated I_P's and E_A's. This material is available free of charge via the Internet at http://pubs.acs.org.

■ AUTHOR INFORMATION

Corresponding Author

*E-mail: michiel.setten@kit.edu.

Notes

The authors declare no competing financial interest.

■ ACKNOWLEDGMENTS

Financial support by the Center for Functional Nanostructures (CFN) and CPU time allocation at the HC3 cluster at the Karlsruhe Institute of Technology (KIT) Steinbuch Center for Computing (SCC) are gratefully acknowledged.

■ REFERENCES

(1) Kohn, W. *Rev. Mod. Phys.* **1999**, *71*, 1253.
(2) Dirac, P. A. M. *Proc. R. Soc. London* **1929**, *A 123*, 714.
(3) Perdew, J. P.; Wang, Y. *Phys. Rev. B* **1992**, *45*, 13244.
(4) Koopmans, T. *Physica* **1934**, *1*, 104−113.
(5) Chong, D.; Gritsenko, O.; Baerends, E. *J. Chem. Phys.* **2002**, *116*, 1760−1772.
(6) Gritsenko, O.; Baerends, E. J. *Can. J. Chem.-Rev. Can. Chim.* **2009**, *87*, 1383−1391.
(7) Hedin, L. *Phys. Rev.* **1965**, *139*, A796.
(8) Hedin, L. *Ark. Fys.* **1965**, *30*, 231.
(9) Hedin, L. *J. Phys.: Condens. Matter* **1999**, *11*, R489.
(10) Aryasetiawan, F.; Gunnarsson, O. *Rep. Prog. Phys.* **1998**, *61*, 237.
(11) Onida, G.; Reining, L.; Rubio, A. *Rev. Mod. Phys.* **2002**, *74*, 601−659.
(12) Huang, P.; Carter, E. A. *Annu. Rev. Phys. Chem.* **2008**, *59*, 261.
(13) Galitskii, V. M.; Migdal, A. B. *Sov. Phys. JETP-USSR* **1958**, *7*, 96.
(14) Sham, L. J.; Schlüter, M. *Phys. Rev. B* **1985**, *32*, 3883−3889.
(15) van Leeuwen, R.; Baerends, E. J. *Phys. Rev. A* **1994**, *49*, 2421.
(16) Baroni, S.; Parravicini, G.; Pezzica, G. *Phys. Rev. B* **1985**, *32*, 4077.
(17) Hybertsen, M. S.; Louie, S. G. *Phys. Rev. B* **1986**, *34*, 5390.
(18) Godby, R.; Schlüter, M.; Sham, L. *Phys. Rev. B Rapid Commun.* **1987**, *35*, 4170.
(19) Bardyszewski, W.; Hedin, L. *Phys. Scr.* **1985**, *32*, 439.
(20) van Gelderen, P.; Bobbert, P. A.; Kelly, P. J.; Brocks, G. *Phys. Rev. Lett.* **2000**, *85*, 2989.
(21) van Schilfgaarde, M.; Kotani, T.; Faleev, S. *Phys. Rev. Lett.* **2006**, *96*, 226402.
(22) Rangel, T.; Kecik, D.; Trevisanutto, P. E.; Rignanese, G.-M.; Van Swygenhoven, H.; Olevano, V. *Phys. Rev. B* **2012**, *86*, 125125.
(23) Kutepov, A.; Haule, K.; Savrasov, S. Y.; Kotliar, G. *Phys. Rev. B* **2012**, *85*, 155129.
(24) Shishkin, M.; Kresse, G. *Phys. Rev. B* **2006**, *74*, 035101.
(25) Shishkin, M.; Marsman, M.; Kresse, G. *Phys. Rev. Lett.* **2007**, *99*, 246403.
(26) Marini, A.; Hogan, C.; Gruening, M.; Varsano, D. *Comput. Phys. Commun.* **2009**, *180*, 1392.
(27) Friedrich, C.; Bluegel, S.; Schindlmayr, A. *Phys. Rev. B* **2010**, *81*, 125102.
(28) Schindlmayr, A.; Friedrich, C.; Sasioglu, E.; Bluegel, S. *Z. Phys. Chem. (Muenchen, Ger.)* **2010**, *224*, 357−368.
(29) Deslippe, J.; Samsonidze, G.; Strubbe, D. A.; Jain, M.; Cohen, M. L.; Louie, S. G. *Comput. Phys. Commun.* **2012**, *183*, 1269−1289.
(30) Umari, P.; Stenuit, G.; Baroni, S. *Phys. Rev. B* **2009**, *79*, 201104.
(31) Berger, J. A.; Reining, L.; Sottile, F. *Phys. Rev. B* **2010**, *82*, 041103.
(32) Kim, Y.-S.; Marsman, M.; Kresse, G.; Tran, F.; Blaha, P. *Phys. Rev. B* **2010**, *82*, 205212.

(33) Shih, B.-C.; Xue, Y.; Zhang, P.; Cohen, M. L.; Louie, S. G. *Phys. Rev. Lett.* **2010**, *105*, 146401.
(34) Gómez-Abal, R.; Li, X.; Scheffler, M.; Ambrosch-Draxl, C. *Phys. Rev. Lett.* **2008**, *101*, 106404.
(35) Grossman, J. C.; Rohlfing, M.; Mitas, L.; Louie, S. G.; Cohen, M. L. *Phys. Rev. Lett.* **2001**, *86*, 472.
(36) Ethridge, E. C.; Fry, J. L.; Zaider, M. *Phys. Rev. B* **1996**, *53*, 3662−3668.
(37) Tiago, M.; Chelikowsky, J. R. *Phys. Rev. B* **2006**, *73*, 205334.
(38) Rostgaard, C.; Jacobsen, K. W.; Thygesen, K. S. *Phys. Rev. B* **2010**, *81*, 085103.
(39) Ke, S. *Phys. Rev. B* **2011**, *84*, 205415.
(40) Blase, X.; Attaccalite, C.; Olevano, V. *Phys. Rev. B* **2011**, *83*, 115103.
(41) Baumeier, B.; Andrienko, D.; Ma, Y.; Rohlfing, M. *J. Chem. Theory Comput.* **2012**, *8*, 997.
(42) Sharifzadeh, S.; Tamblyn, I.; Doak, P.; Darancet, P. T.; Neaton, J. B. *Euro. Phys. J. B* **2012**, *85*, 323.
(43) del Puerto, M. L.; Tiago, M.; Chelikowsky, J. R. *Phys. Rev. Lett.* **2006**, *97*, 096401.
(44) del Puerto, M. L.; Tiago, M.; Chelikowsky, J. R. *Phys Rev. B* **2008**, *77*, 045404.
(45) Ramos, L.; Paier, J.; Kresse, G.; Bechstedt, F. *Phys Rev. B.* **2008**, *78*, 195423.
(46) Pavlyukh, Y.; Hübner, W. *Phys. Lett. A* **2004**, *327*, 241.
(47) Noguchi, Y.; Ishii, S.; Ohno, K.; Sasaki, T. *J. Chem. Phys.* **2008**, *129*, 104104.
(48) Bruneval, F. *Phys. Rev. Lett.* **2009**, *103*, 176403.
(49) Tiago, M. L.; Idrobo, J. C.; Öğüt, S.; Jellinek, J.; Chelikowsky, J. R. *Phys. Rev. B* **2009**, *79*, 155419.
(50) Adachi, H.; Ishii, S.; Ohno, K.; Ichinoseki, K.; Kawazoe, Y. *Mater. Trans.* **2006**, *47*, 2620−2623.
(51) Stan, A.; Dahlen, N. E.; van Leeuwen, R. *J. Chem. Phys.* **2009**, *130*, 114105.
(52) Ren, X.; Rinke, P.; Blum, V.; Wieferink, J.; Tkatchenko, A.; Sanfilippo, A.; Reuter, K.; Scheffler, M. *New J. Phys.* **2012**, *14*, 053020.
(53) Thygesen, K. S.; Rubio, A. *Phys. Rev. B* **2008**, *77*, 115333.
(54) Thygesen, K. S.; Rubio, A. *Phys. Rev. Lett.* **2009**, *102*, 046802.
(55) Foerster, D.; Koval, P.; Sanchez-Portal, D. *J. Chem. Phys.* **2011**, *135*, 074105.
(56) Bruneval, F. *J. Chem. Phys.* **2012**, *136*, 194107.
(57) Blum, V.; Gehrke, R.; Hanke, F.; Havu, P.; Havu, V.; Ren, X.; Reuter, K.; Scheffler, M. *Comput. Phys. Commun.* **2009**, *180*, 2175−2196.
(58) Tiago, M. L.; Chelikowsky, J. R. *Solid State Commun.* **2005**, *136*, 333.
(59) Abrikosov, A. A.; Gorkov, L. P.; Dzyaloshinski, I. E. *Methods of quantum field theory in statistical physics*; Dover Publications: New York, 1963; p 51.
(60) Lehmann, H. *Nuovo Cimento* **1954**, *11*, 342.
(61) Caruso, F.; Rinke, P.; Ren, X.; Scheffler, M.; Rubio, A. *Phys. Rev. B* **2012**, *86*, 081102.
(62) Tandetzky, F.; Dewhurst, J. K.; Sharma, S.; Gross, E. K. U. *arXiv.org, e-Print Arch., Condens. Matter* **2012**, *1205*, 4274.
(63) Furche, F.; Ahlrichs, R. *J. Chem. Phys.* **2004**, *121*, 12772−12773.
(64) Hybertsen, M. S.; Louie, S. G. *Phys. Rev. Lett.* **1985**, *55*, 1418−1421.
(65) Godby, R. W.; Schlüter, M.; Sham, L. J. *Phys. Rev. Lett.* **1986**, *56*, 2415−2418.
(66) Bohm, D.; Pines, D. *Phys. Rev.* **1952**, *85*, 338.
(67) Bohm, D.; Pines, D. *Phys. Rev.* **1953**, *92*, 609.
(68) Casida, M. *In Recent Advances in Density Functional Methods, Part I*; World Scientic: Singapore, 1995; pp 155−192.
(69) Eichkorn, K.; Treutler, O.; Oehm, H.; Haeser, M.; Ahlrichs, R. *Chem. Phys. Lett.* **1995**, *240*, 283.
(70) Weigend, F. *Phys. Chem. Chem. Phys.* **2006**, *8*, 1057.
(71) Weigend, F.; Ahlrichs, R. *Phys. Chem. Chem. Phys.* **2005**, *7*, 3297.
(72) Perdew, J.; Parr, R.; Levy, M.; Balduz, J. *Phys. Rev. Lett.* **1982**, *49*, 1691−1694.
(73) Perdew, J.; Levy, M. *Phys. Rev. Lett.* **1983**, *51*, 1884−1887.
(74) Perdew, J. P.; Levy, M. *Phys. Rev. B* **1997**, *56*, 16021−16028.
(75) Dirac, P. *Proc. R. Soc. London, Ser. A* **1929**, *123*, 714.
(76) Slater, J. *Phys. Rev.* **1951**, *81*, 385.
(77) Perdew, J.; Wang, Y. *Phys. Rev. B* **1992**, *45*, 13244.
(78) Perdew, J.; Burke, K.; Ernzerhof, M. *Phys. Rev. Lett.* **1996**, *77*, 3865.
(79) Vosko, S.; Wilk, L.; Nusair, M. *Can. J. Phys.* **1980**, *58*, 1200.
(80) Becke, A. *Phys. Rev. A* **1988**, *38*, 3098.
(81) Lee, C.; Yang, W.; Parr, R. *Phys. Rev. B* **1988**, *37*, 785.
(82) Becke, A. *J. Chem. Phys.* **1993**, *98*, 5648.
(83) Cederbaum, L. S.; Hohlneicher, G.; Niessen, W. *Chem. Phys. Lett.* **1973**, *18*, 503.
(84) Pang, W.; Shang, R.; Gao, J.; Gao, N.; Chen, X.; Deleuze, M. *Chem. Phys. Lett.* **1998**, *296*, 605.
(85) Deleuze, M.; Cederbaum, L. *J. Chem. Phys.* **1996**, *105*, 7583−7596.
(86) Gritsenko, O.; Baerends, E. *J. Chem. Phys.* **2002**, *117*, 9154−9159.
(87) Fuchs, F.; Furthmüller, J.; Bechstedt, F.; Shishkin, M.; Kresse, G. *Phys. Rev. B* **2007**, *76*, 115109.
(88) Rinke, P.; Qteish, A.; Neugebauer, J.; Freysoldt, C.; Scheffler, M. *New J. Phys.* **2005**, *7*, 126.
(89) Here we make a strict distinction between G_H and G_{in}, which are in the *GW*-literature often both denoted by G_0. We find this nomenclature misleading however since in the general literature of quantum field theory G_0 refers to the Green's function of a strictly noninteracting reference system, i.e., also without mean-field interaction.
(90) For single-particle ground states (single Slater determinant) the pole positions and residues of the Green's function do not depend on z. By contrast, for ground states with more than a single Slater determinant, pole positions and residues in general do depend on z. The z-dependency takes into account that the spectral-function $A(E)$ of interacting electron gases is not just a superposition of N Lorentzians. We add that G has a second spectral representation in terms of a sum over all the many-body states of the electron gas. In this representation the poles do not depend on z; the price to be paid for this simplification is that the number of poles appearing is not given by the number of particles, N, but by the much larger number of all many-body excitations.
(91) *Alternative derivation.* One can also understand the quasi-particle equation, 25, from a slightly different point of view, where the reference Hamiltonian in the constituting equations 1−5 is not the Hartree one but the KS-Hamiltonian: $H_H \rightarrow H_{KS}$. In this case we will find

$$\sum_{\bar{n}} \mathcal{U}_{n',\bar{n}}(z)[\varepsilon_n \delta_{n,\bar{n}}] = \varepsilon_{n'}(z)\ \mathcal{U}_{n',n}(z)$$

where the self-energy now is with respect to the residual interactions not yet included in V_{HXC}. This expression is identical with eq 25 because for it the Hedin equations should be reformulated in terms of the residual interactions and then solved self-consistently. In practical terms this is done by dressing all Green's functions appearing in the expressions for Σ_{KS} with local-potential insertions V_{XC}. This dressing, effectively, reconverts Σ_{KS} into the original object Σ plus a shift which is V_{XC}, see eq 25.
(92) The poles reside in the upper and the lower complex half planes. This representation is inherited from the fact that the constituting equations refer to causal Green's functions.
(93) For some of the smaller molecules values do exist at fully self-consistent *GW*-level.[38] Since however these form only a small subset we prefer to stick in our comparison to the experimental values as a reference.
(94) This is in accordance with the analysis in ref 86 which concludes that the KS-levels are approximations to the ionization potentials up to a shift that is constant within an electronic shell. (The same observation can be made for H_2O and N_2; there however the trend is less obvious due to the limited amount of data points.)
(95) The only exception is SF4. Here even between TZVPP and QZVP the KS-energy levels change by more than 0.1 eV.
(96) The SSD is calculated in the usual way as $s = ((1)/(N-1)\Sigma_{i=1}N\text{-}(x_i - \bar{x})^2)^{1/2}$ with $\bar{x} = (1)/(N)\Sigma_i x_i$.
(97) Both benzene and naphthalene were calculated using "really tight Tier 2" settings since the use of a Tier 3 basis set led in these cases to an overcomplete basis set.